ABSTRACT

ALEXANDER PRINTZIOS

SUPPRESSION OF WIND-INDUCED OSCILLATIONS IN STEEL STACKS

The subject of this thesis examines the phenomenon of wind-induced oscillations in tall metal chimney stacks.

Possible sources of these oscillations are discussed, with emphasis on the periodic mechanism involving vortex shedding.

The effectiveness of existing methods for suppressing oscillations due to vortex shedding are examined with emphasis on aerodynamic and damping devices.

Based on existing experimental results, the most effective use of these devices is formulated in a manner intended primarily for the practicing structural engineer.

Finally, it was found, that most aerodynamic devices are almost equally effective and that more research is needed to clarify certain areas associated with the wind-induced oscillations and their suppression.

ACKNOWLEDGEMENTS

ACKNOWLEDGEMENTS

The sincere qratitude of the author is extended to his research supervisor Dr. M.S. Troitsky, Professor of Engineering and Chairman of the Department of Civil Engineering, for his invaluable guidance and encouragement which proved extremely valuable troughout the course of this work.

TABLE OF CONTENTS

TABLE OF CONTENTS

LIST OF TABLES

LIST OF TABLES

LIST OF FIGURES

LIST OF FIGURES

NOTATIONS

NOTATIONS

a	Power-law exponent
C_L	Lift coefficient
C_D	Drag coefficient
CM	Accepted concentration of SO_2 at ground level
c_o	Chord length
C_R	Design rigidity of the guys
D	Diameter
e	Elongation
e_t	Change in length due to temperature
f_d	Damped natural frequency
f_o, f_n	Natural frequency
f_s, f_{vs}	Vortex shedding frequency
F(z)	Fluctuating force at height (z)
H	Height
$H_{(f)}$	Mechanical admittance function in terms of frequency f
$H_{(\omega)}$	Mechanical admittance function in terms of circular frequency
H_o	Horizontal component of the reaction at the upper end of a guy
K	Von Karman constant
k	Structural stiffness parameter
k_a	Aerodynamic damping coefficient
L_o	Arc length
m	Structural mass per unit length
P(x)	Probability density function
P(a)	Maximum probability density function
Q	Weight of SO_2 contained in smoke, in Kg/h
q_o	Gravity load per unit length

R	Smoke volume at the chimney top in true m^3/h
Re	Reynolds number
S	Strouhal number
$S_{xx(\omega)}$	Spectral density function of $F_{(t)}$
t	Time parameter
T	Time period
T_m	Tension at point m
V_1	Reference wind speed
V_g	Gradient wind velocity
V	Fluid velocity
V_o	Vertical component of the reaction at the upper end of the guy
V_r	Reduced velocity
$\bar{V}(z)$	Mean wind velocity at height z
V^*	Friction velocity
W	Wind load
w	Relative flow velocity
Z_o	Length dependent on surface roughness
Z_1	Reference height
α	Angle between chord and horizontal
Δ	Cable initial sag
δ	Logarithmic increment
ΔL	Change in arc length
ΔT	Difference between the temperature of the smoke or fumes at the chimney top and of the taken air temperature equal to 15° C
ε_t	Coefficient of thermal expansion
ζ	Damping ratio

η	Ratio of maximum linear displacement from the zero position during a period of oscillation over the diameter of the stack
θ	Angle at which flow separation occurs
ν	Kinematic coefficient of viscosity
σ	Variance
$\sigma^2(x)$	Mean square value of random response
Φ_f	Argument or phase angle of admittance function $H(f)$
$\Phi(\omega)$	Phase angle
$\Phi(x)$	Power spectral density function
λ	Exponent used in Equation 4.3

CHAPTER 1

INTRODUCTION

1.1 GENERAL INTRODUCTION

One of the principal problems in air-quality control is the discharge of gaseous industrial wastes near or around heavily populated areas.

The rapid growth of industrial activity in recent years coupled with Government imposed strict environmental regulations created the need for higher and more slender stacks in order to prevent excessive air pollution at ground level. Hence, in several countries these regulations were incorporated into the existing standards dealing with the design of industrial stacks.

The British Standard 4076 and the German DIN 1056 are good examples. However, the French regulations for industrial chimneys may be regarded as the most advanced in dealing with stack height. In France, until 1970, no law existed imposing stack heights. These were calculated in order to obtain the necessary draught without the use of ventilators. With the appearance of powerful installations, such as thermal power stations of 500 to 2,800 M.W., and the generalized use of heavy fuel no. 2 with 4% sulphur, it was realised that industrial stack height would have to be regulated. The "circular of the 24th November 1970 relating to chimney construction for combustion installations, slightly modified by the decree of the 20th June 1975" sets firstly a minimum chimney height in order to limit ground level pollution: [1,2]

$$H = \sqrt{\frac{340Q}{CM}} \sqrt[3]{\frac{1}{R(\Delta T)}} \qquad (1.1)$$

Similarly, in N. America considerable attention has been given to the subject especially after the recent formation of powerful groups of environmentalists monitoring all sources of pollution around heavily populated areas.

The need for increased height in stacks introduced certain stability problems as it has made these structures more susceptible to the wind - excited oscillations.

Although it has been well known that wind forces can cause high stacks to oscillate, complete information on their aerodynamic behaviour has not been yet fully clarified.

However, up to now, attention seems to have been paid only to the stability problems of determining the critical wind velocity for the aeroelastic instability of structures.

From the point of view of structural design, the oscillatory amplitude is of main interest so that the response problems may be considered.

In aerodynamic terms the earth's surface wind is a boundary layer which, typically, is in the range 900 to 1,500 ft. thick. The flow in the layer is complex because of the interactions with the earth's surface. The velocity increases with height and is highly turbulent or gusty. The physical scales and time scales of the turbulence fluctuations are such that they are important in the aerodynamic behaviour of many civil engineering structures from the point of view of wind loads, surface pressures and vibration.

Distinct from the vibrations due to the wind turbulence, there are many slender engineering structures, both large and small, that are prone to wind-unduced vibration because of aeroelastic instabilities that arise due to the sectional geometry of the structure itself. In the case of cylindrical steel stacks, a steady wind flow induces lateral vibrations due to the formation of vortices on alternating sides of the stack. These vortices are formed and shed from opposite sides of the stack at a regular frequency, depending on the velocity of the wind and as a result alternating lateral forces are exerted by the wind motion. When the frequency of vortex shedding (and hence the frequency of the alternating forces) is approximately equal to the frequency of one of the normal modes of vibration of the stack, then, depending on the properties of the stack and the nature of the incident flow, the stack may respond dynamically and relative large across - flow oscillation amplitudes can occur.

If the structural damping and the stiffness of the stack are small and the wind remains steady, large amplitudes of vibration will be developed.

These vibrations possess the ability of self-exciting for a limited range of wind velocities at and around the "critical" wind velocity. This self-amplification has an upper limit of vibrational stability, so that the vibrations produced by the wind are not catastrophic in nature.

Oscillations persists for a certain range of wind speed above the critical velocity and reaches a maximum amplitude near the top of the range.

There are several methods by which vibrations of this type can be suppressed:

1. By increasing the flexural stiffness of the member so that its critical velocity is above the range of moderate winds;
2. By reducing the effective length of the stack through the introduction of intermediate struts;
3. By use of damping devices to restrict the amplitude of vibration; or
4. By introducing "aerodynamic devices" to the stack that serve to disrupt the flow near the surface and to interfere with the regular formation of vortices, hence destroying the cause of the vibrations.

In the past, the first three methods of suppressing wind - induced vibrations have been used extensively. However, practical limitations due to height increase requirements led to the investigation into the possible application of devices that were used only in aerospace industry as means of improving the stability and control of aircraft structures. The idea originated from the fact that in both, aerospace and civil engineering structures, the behaviour of wind flow is similar.

The investigation of the possible use of aerodynamic devices commenced with the problem of wind-induced vibrations in individual members of large radar antenna space frames.

Several failures have been attributed to the action of Von Karman Vortex forces. The failures occured in slender tubular members subjected to moderate winds, and they were observed to be fatigue - type failures in weld-heated areas at points of maximum flexural stresses. Similar failures in steel stacks, prompted designers to investigate the problem as it was becoming very serious.

In general, failure of a stack may be broadly classified as structural failure or as seryiceability failure, the latter including both operational and environmental problems. Unsteady wind loading may contribute to any of these and it is often found that serviceability problems impose more stringent limits than structural failures.

When a steel stack does not oscillate significantly in response to fluctuating loading, that loading may be a significant part of the total. The applied loading can be considerably amplified by inertia effects and the resulting stresses are then much higher than for static loading of similar magnitude. This may lead to direct failure due to overstressing. Excessive relative motion between individual structural components, caused by

oscillation, may lead to collapse or cracking of joints and cladding. Fluctuating deflections can lead to wear failures such as for heat exchanges tubes passing through closely fitting baffles.

Individual structural members of a steel stack subjected to repeatedly varying loading may fail, due to fatigue, at stresses well below the static failure stress. Where the loading cycle can be precisely defined it may be possible to estimate fatique life. For random loading a very high uncertainty in the calculated life is inevitable and limiting the stresses to below the fatigue limit (where fatigue life is effectively infinite) may be preferable. Joints are particularly susceptible to failure due to repeated loading because of fatigue of welded areas and fatigue or loosening of other fasteners.

The aim of this study is to investigate the effectiveness of various methods of suppressing wind-induced vibrations with emphasis on aerodynamic devices.

Although, experimental investigation is required in obtaining conclusive results, it is not necessary to undertake experimental work due to the fact that sufficient experimental data is already available through past laboratory studies in most areas of the subject.

The main objective in this study is to formulate the problem and provide practical solutions in a manner understandable and most usefull to the practicing structural engineer encountering design problems due to wind effects in tall steel stacks.

1.2 HISTORICAL BACKGROUND

The nature of wind-induced stack vibrations was first established through observations on the stacks of the Congress Street Heating Plant [3], and was later substantiated on other steel stacks. As a result, an investigation was undertaken to determine the amount and the structural significance of the movement in the interests of safety and public relations.

Of the reported cases of full scale stack vibration the problem of swaying has proved to be the most serious. Several cases of large amplitude oscillations have been observed. One such incident is described by Dickey and Woodruff. [4]

In this incident two large stacks located in Baltimore underwent large amplitude vibrations at 2.2 cycles/sec. with wind speeds of 53 mph.

The stacks were 11 ft. in diameter and had a wall thickness varying from ¼ in. to 5/16 in.

Another similar incident occured in Guam in a single stack at 105 cycles/min. with wind speeds of up to 125 mph. The stack was 150 ft. high, 9 ft. in diameter and had a wall thickness varying from ⅜ to ½ in.

A case in which large amplitude ovalling resulted in the collapse of a chimney stack is described by Sharma and Johns [5].

The stack was 150 ft. high, 10 ft. in diameter and had a wall thickness of 5/16 in. The large amplitude vibrations which occured at 1.6 - 2.4 Hz was filmed during a typhoon. The large vibrations caused a ring stiffner to

break away resulting in increased amplitude vibrations and the eventual collapse of the structure.

These are only a few of the numerous incidents in vibrations of steel stacks. Very little can be concluded as to the exact cause of these vibrations because of the lack of accurate measurements of wind velocity, vibration frequency and natural frequency of vibration. Rough estimates of the wind velocity and natural frequencies of vibration have led many researchers to suspect vortex shedding as the cause of wind induced oscillations.

Vortex shedding refers to the periodic shedding of local concentrations of vorticity resulting from the alternate rolling up to the two layers of vorticity which separate from opposite sides of the cylinder.

The shedding of these vortices results in periodic lift and drag forces acting on the cylindrical structure and it has been shown that this periodic force can result in swaying oscillations when the frequency at which the vortices are shed corresponds to the natural frequency of sway vibrations.

A large number of studies have examined the problem of vibrations arising from the periodic force resulting from vortex shedding. Some of the more notable work has been conducted by Davenport [6] , Vikery and Watkins[7] , Scruton [8], Ferguson and Parkinson[9] and Novak and Tanaka [10].

As a direct result of these studies, was the consideration of several mechanical and aerodynamic devices as means for suppressing vortex-induced oscillations.

Hence, Scruton and Walshe[11] , during experimental studies at National Physical Laboratory - England, developed a device of a number of projections, or strakes, wound as helices round the external surfaces of the cylinder. Further experimental studies by Woodgate and Maybrey[12] , found later that a 3 - start system with strakes wound with a helix-pitch of about 5D was the best arrangement and changed the aerodynamic excitation of a circular cylinder to a positive aerodynamic damping. More recent studies by Cowdrey and Lawes [13] and Walshe and Cowdrey have been indicating successful results in reducing large amplitude oscillations. [14]

Price, [15] demonstrated experimentally that regular vortex shedding from a cylinder can be prevented by fitting a perforated shell or shroud round the cylinder, but separated from it by a gap. Similar investigations by Walshe[16] Knell [17] and Wooton and Yates [18] have shown that neither the gap width nor the open - area ratio is very critical but that a gap width of 0.12D and an open - area ratio between 20% and 36% are the most effective. Stability was obtained with only the top 25% of the model height shrouded which was found sufficient in preventing oscillations in the fundamental mode of bending of full scale stacks.

Wind - tunnel tests carried out on circular cylinders fitted with spoilers were conducted by Novak [19] and the results were encouraging. Following these tests a tower was built in Bukova hora (designer Ing. Marten) and fitted with steel - sheet spoilers welded normal to the cylinder surface in order to disturb the flow past the cylinder [20]. They have proved well according to the follow-up observations.

In the area of mechanical devices most of the work was concentrated into the design and testing of various dampers.

Dampers have come into use not so long ago and a lot of papers are devoted to them. They can, evidently, be used to damp vibrations of tower structures in a wind flow.

The first dampers which are known on towerlike structures were installed in 1951 on six chimneys of the Transcaucasion metalurgical plant in the town of Rustavi (USSR). [21]

However, most of the work on dampers was carried out by Korenev from Central Research Institute for Building Structures of the USSR. [22]

It was his idea the introduction of impact and tunned dampers. Walshe and Wooton [23] and later Wong [24] investigated the effectiveness of another type of dampers namely active mechanical dampers or viscous dampers - force producing devices on the structure, opposing the wind dynamic force.

Presently, due to the seriousness of the problem of wind induced oscillations in steel stacks, extensive work is being under-way in various countries. In Canada both, the National Research Council and the University of Western Ontario with

their modern experimental facilities are leading the way in the investigation of various methods for reducing wind induced oscillations in steel staks.

CHAPTER 2

WIND PROPERTIES

2.1 THE NATURAL WIND MEAN VELOCITY PROFILE

Air movement accross the earth forms what is in effect a turbulent boundary layer to a stationary observer, this takes the form of a wind of fluctuating velocity and direction.

The mean velocity increases with height from a low value near the ground to what may be termed the free stream velocity of height ranging from 900 to 1,500 ft.

The flow in this layer is complex due to the interactions with the earth's surface.

Experimentaly, [25,26] it has been found that there exists a relationship between the mean wind velocity and height given as:

$$\frac{\bar{V}(z)}{V^*} = \frac{1}{K} \ln \frac{(Z + Z_o)}{Z_o} \qquad (2.1)$$

Values of Z_o can range from 1×10^{-5}m. for mud flats, ice, etc. to 1×10^{-3}m. for lawn grass, 1×10^{-2}m. for tall thick grass, 1 m. for woodlands, 1 to 5 m. for urban areas.

However, Equation (2.1) assumes a constant roughness fetch. In practical situations this is not always the case as with wind approaching an urban centre. Davenport [27] gives an example of wind blowing from flat open terrain to a suburban terrain. For the new boundary layer to establish itself to a height of 100 feet requires a downstream distance of approximately 3/4 mile from the change of roughness.

A more popular profile law for use in wind effects engineering is the power law.

$$\frac{\bar{V}(z)}{V_1} = \frac{z}{z_1}^{a} \qquad (2.2)$$

The log law (Eqn. 2.1) describes approximately the lower third of the boundary layer outside the region directly influenced by the roughness elements. The power law, (Eqn. 2.2) while having no analytical basis, is often preferred because of its wider applicability across the layer and because of its convenience.

For the reference wind speed, V_1, it is convenient to use the geostrophic or "gradient" wind velocity, V_g. This wind speed is attained above the layer of frictional influence and is governed only by pressure gradients.

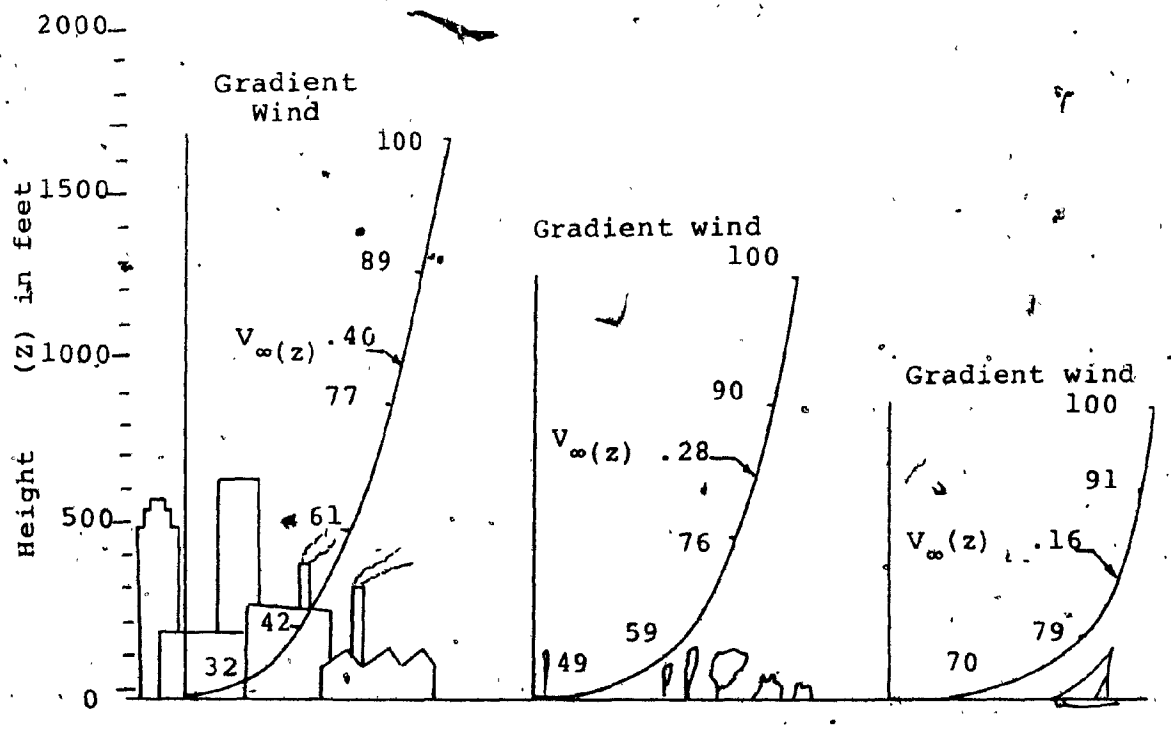

Figure 2.1 Natural Mean Wind Profiles.

The reference height, Z_g, will then be the height at which V_g is attained. Typical urban, suburban and open country profiles are shown in Figure 2.1 and Figure 2.2. The gradient height ranges from about 900 feet for smooth terrain to 1,500 or 2,000 feet for urban terrain.

The exponent, a, varies from about 0.16 for smooth terrain to 0.4 for urban terrain. The Canadian National Building Code defines three standard terrains:

Exposure A - Open level terrain with only scattered buildings, trees or other obstructions, open water or shorelines thereof.

Exposure B - Suburban and urban areas, wooded terrain, or centres of large towns.

Exposure C - Centres of large cities, with heavy concentrations of tall buildings. At least 50 percent of the buildings should exceed four storeys.

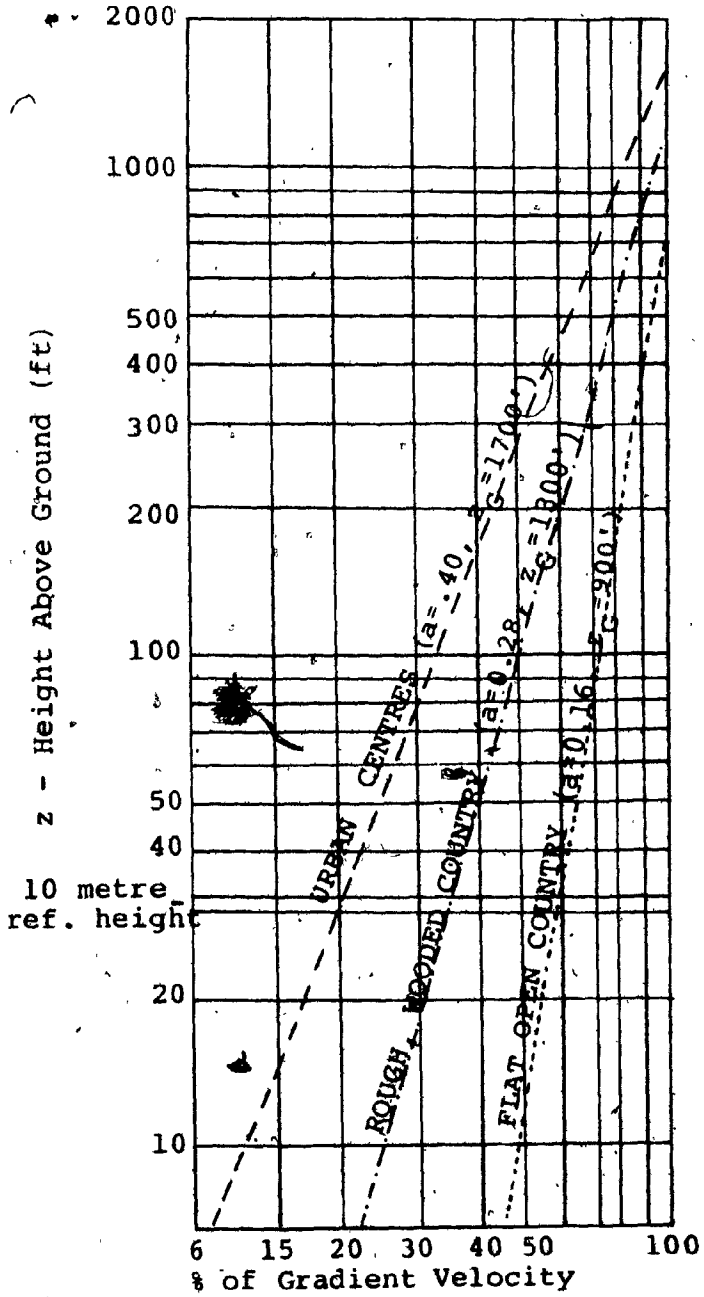

Figure 2.2 Natural Wind Velocity Profiles [28]

Exposures

B and C should not be used unless the appropriate terrain persists in the upwind direction for at least one mile. For these exposures they specify values of a = 0.14, 0.25 and 0.36 respectively.

2.2 TURBULENCE INTENSITY IN THE NATURAL WIND

Treating the wind as a boundary layer, it can be expected that the turbulence intensity will be constant in the lower 1/3 or 1/4 of the layer where the profile of mean longitudinal intensity would be described by the logarithmic law. If we express the r.m.s. intensity $(\bar{v}^2)^{\frac{1}{2}} = v^1$ as a fraction of the velocity at the edge of the layer, V_g, or in the wind tunnel V, then it is found that for open country

$$\frac{V_1(z)}{V_g} = 10 \text{ percent} \qquad (2.3)$$

or as a fraction of the local mean velocity

$$\frac{V_1(z)}{V(z)} = 10 \text{ to } 20 \text{ percent} \qquad (2.4)$$

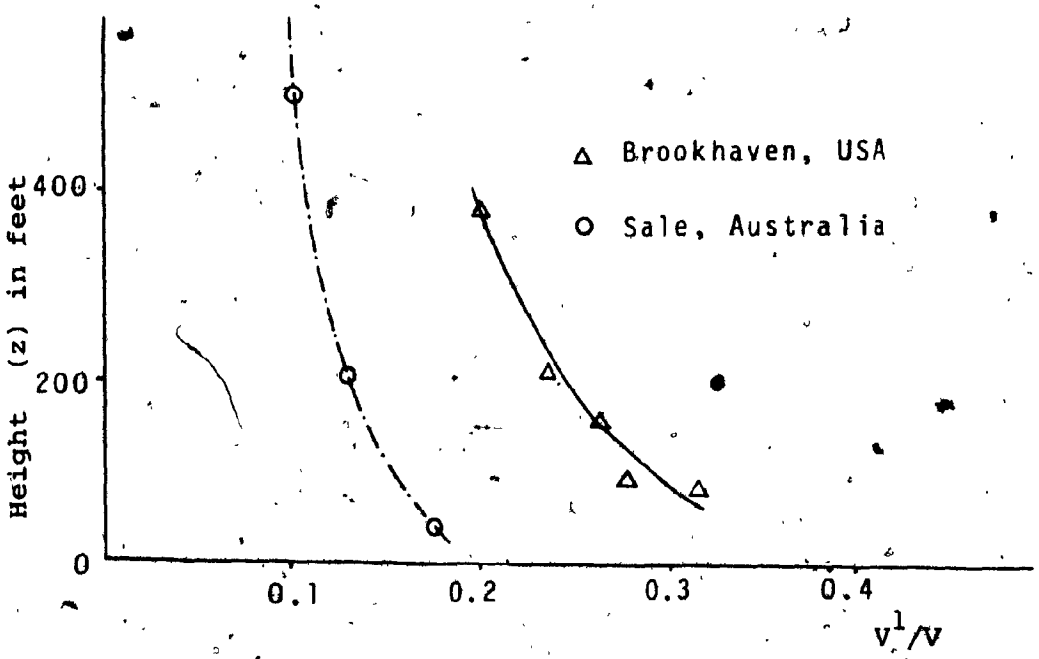

Figure 2.3 Turbulence Intensity in Natural Wind.

Typical values are shown in figure 2.3 [29]for urban areas higher values are expected and

$$\frac{V_1(z)}{V(z)} \qquad 20 \text{ to } 30 \text{ percent} \qquad (2.5)$$

The profiles shown in Figure 2.4 show measurements by Harris [26] of profiles in open country and intensities are predicted using Harris' expression for the turbulence spectra. This shows clearly the effect of terrain and height on turbulence intensity.

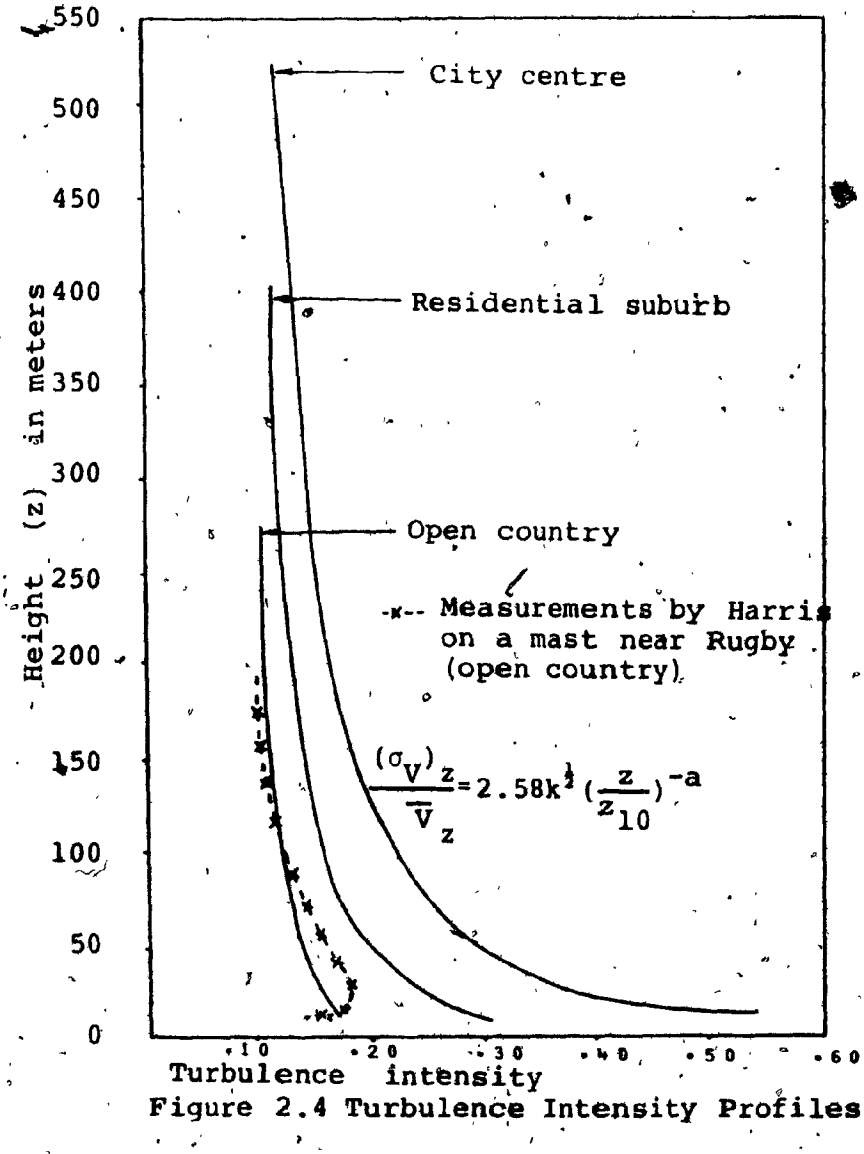

Figure 2.4 Turbulence Intensity Profiles

2.3 WIND TUNNEL SIMULATION OF THE NATURAL WIND

There are several approaches to modelling the wind layer. One attractive approach is to use a long upstream fetch where roughness blocks are placed on the floor which produce after several hundred roughness heights a thick boundary layer which reproduces in a natural way all the wind turbulences and shear properties that are required. The difficulty of this approach is that it requires a special wind tunnel having a suitably long working section. Such facilities exist at the University of Western Ontario and Colorado State University and are extensively used for commercial testing. Such special purpose wind tunnels are not always available and it is desirable to be able to take advantage of existing aeronautical facilities which typically have working sections that are only about twice as long as they were wide, compared to a factor of about ten required to create a good thick boundary layer using floor roughness elements. Techniques for developing artificial or synthetic boundary layers have been devised at a variety of research establishments [28]. These typically incorporate some form of drag device placed accross the entrance to the working section to a height equal to the desired boundary layer thickness.

Figure 2.5 compares the profile of mean velocity to a power law profile with $a = 0.36$. Fig. 2.6 compares the spectrum to measured values for Montreal and the Von Karman spectrum. [29]

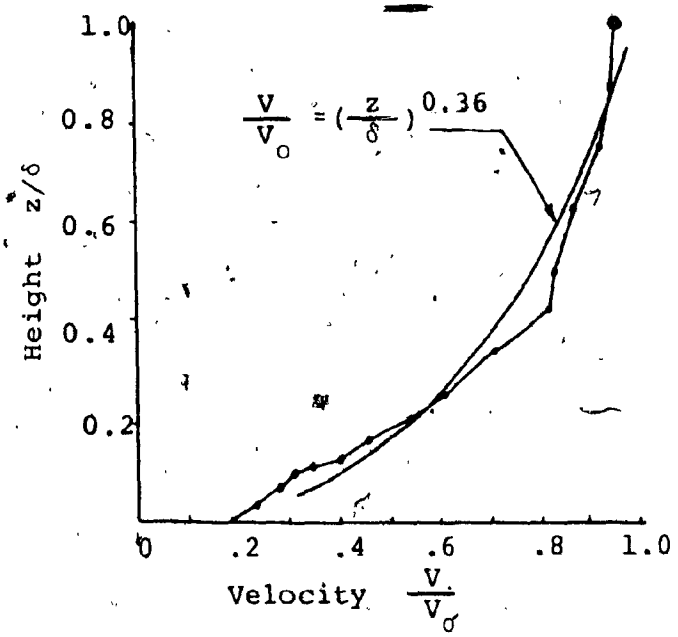

Figure 2.5 Vertical Distribution of Mean Wind Speed

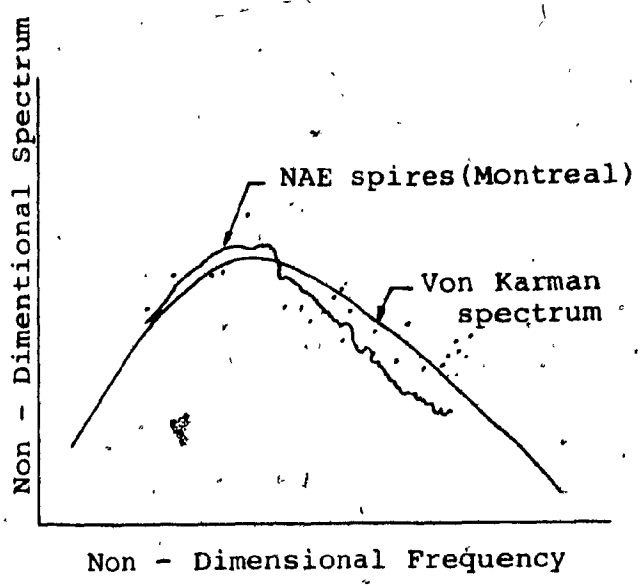

Figure 2.6 Spectrum of Longitudinal Velocity Fluctuations

It is possible to reproduce only the lower part of the layer, thus allowing a larger model scale. For full simulation with a layer of 1,200 ft. a model layer of 3 ft., say, would give a model scale of 1:400. If the top part of the layer above the structure was ignored and only the lower 600 ft. was modelled, then in the same wind tunnel model scales as large as 1:100 could be obtained. The technique is to get the velocity profile with a grid of rods and the turbulence with a coarse rectangular grid. This arrangement is shown in figure 2.7. With this approach the lower frequency portion of the spectrum, that is, the large wavelength eddies, are excluded from the spectra. It is desirable that the spectra at model scale match the atmospheric spectra as shown in Figure 2.8 where only the

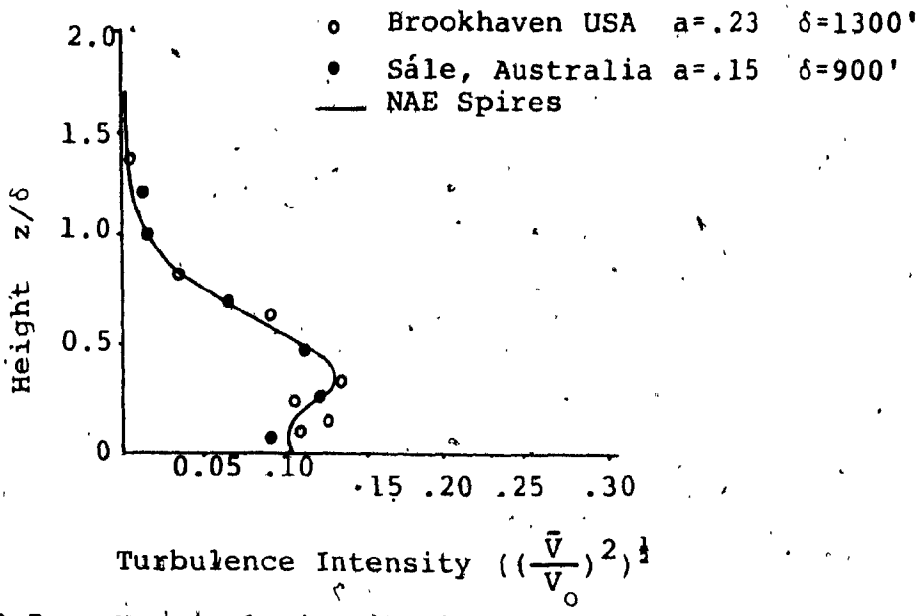

Figure 2.7 Vertical Distribution of Streamwise Turbulence Intensity

higher frequency portions coincide. An argument for this approach can be made if the natural frequencies of the structure under test coincide with the high frequency region where the two spectra are in agreement.

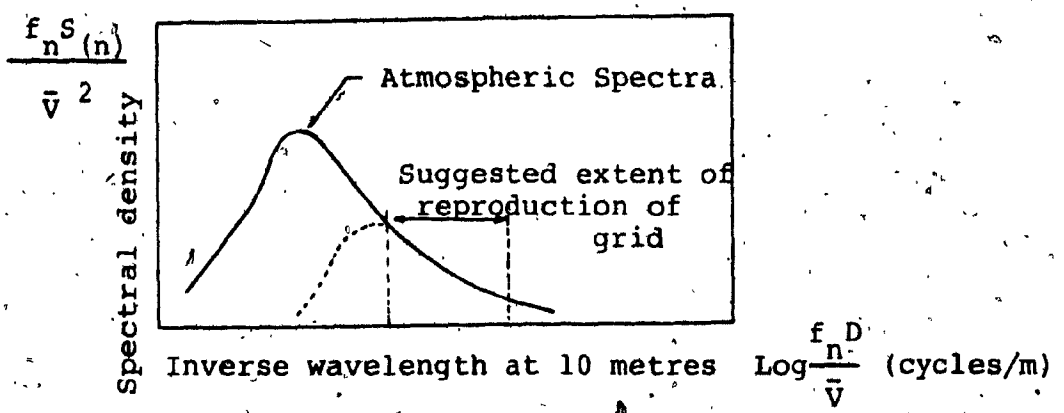

Figure 2.8 Required Spectra for Partial Simulation [31]

2.4 PREDICTION OF WIND LOADS

2.4 (i)- The Mechanical Admittance Function

If $\Phi_f(f)$ is the power spectral density function of the force input to a system, say the force due to the wind, then it can be related to the spectrum of the output, $\Phi_x(f)$ by the relation.

$$\frac{\Phi x(f)}{\Phi_f(f)} = \frac{|H(f)|^2}{k^2} \qquad (2.6)$$

This relationship is shown in Figure 2.9 [31]

The function H(f) is essential in predicting dynamic behaviour. It is dependent on the intensity of the turbulence,

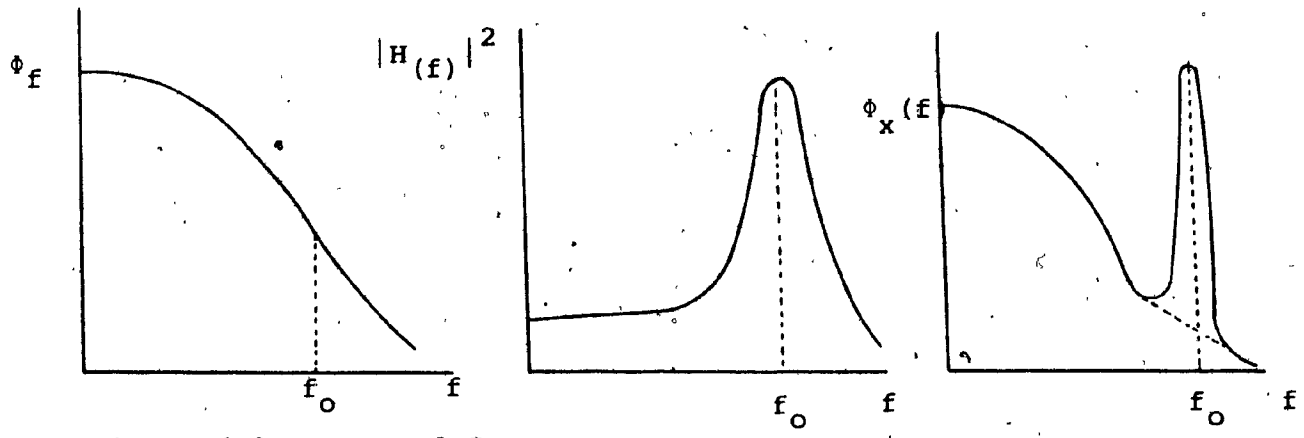

Figure 2.9 Spectral Response

the scale of the turbulence compared to the size of the structure, and on the terrain. It has been possible to make simplifying assumptions that allow H(f) to be evaluated and this is the basis of the dynamic approach in the Canadian National Building Code. [32] The method appears to be in good agreement with measurements made in wind tunnels.

2.4 (ii) Prediction of Extreme Values of Response

The probability density function, p(x), that applies to wind velocity and to a satisfactory extent to wind pressure or force is the Gaussian distribution

$$P(x) = \frac{1}{(2\pi\sigma)^{\frac{1}{2}}} e^{-\frac{x^2}{2\sigma^2}} \qquad (2.7)$$

where $\sigma^2 = (\bar{x}^2)$ (the variance).

The output from a linear system with x as the input will also be Gaussian. The probability distribution of the maximum (or envelope) of a narrow band response (fig. 2.10), which is Gaussian, can be shown to be the Rayleigh Distribution

$$P(a) = \frac{a}{2} e^{-\frac{a^2}{2\sigma^2}} \qquad (2.8)$$

where a is the value of a maximum / and is the variance of x(t)

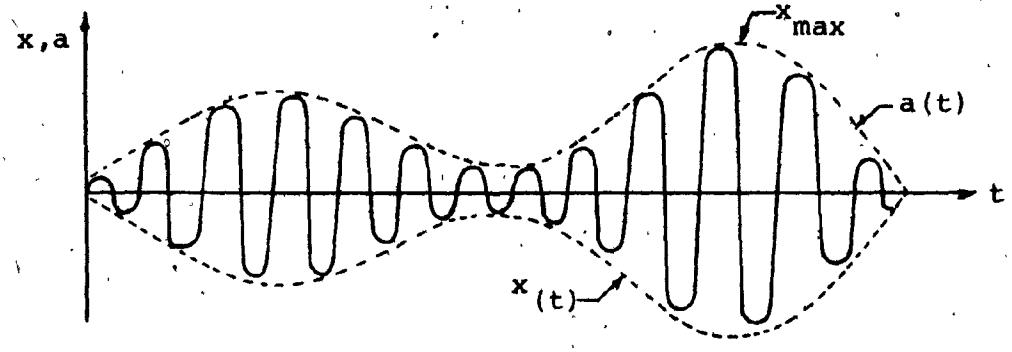

Figure 2.10 Narrow Band Response Maximum

This concept has led to the prediction of maximum deflections used in the Building Code. The maxima are themselves random in character, but their probability density function is narrow as shown in Figure 2.11.

It has been shown by Davenport [33] that, over a large number of samples, the mean value of Xmax is

$$\frac{\bar{X}\ max}{\sigma} = \sqrt{2 \log_e f_o T} + \frac{0.577}{\sqrt{2 \log_e f_o T}} \qquad (2.7)$$

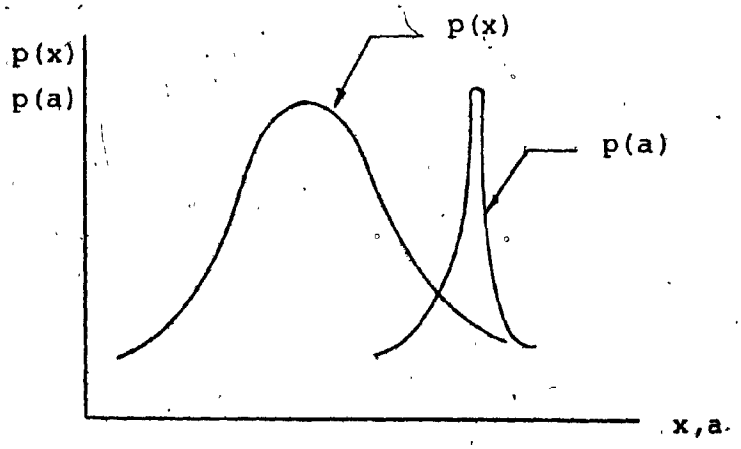

Figure 2.11 Probability Density of System Output

where T is the sample length and

$$f_o = \{\int_o^\infty f^2 \Phi(f) d(f)\}^{\frac{1}{2}} / \int_o^\infty \Phi(f)\ d(f) \qquad (2.8)$$

CHAPTER 3

DYNAMIC WIND EFFECTS

3.1 REVIEW OF WORK ON FLUID FLOW ABOUT A CIRCULAR CYLINDER

Prior to examining the dynamic wind effects on steel stacks with circular cross-section here it may be appropriate to discuss in general the behaviour of fluid flow about a circular cylinder.

Osborne Reynolds, an English physicist, was the first who made an intensive study of flow of air at different speeds around objects of varying size.

Experimentally, he found that at low speeds the flow was smooth but at high speeds the flow was turbulent.

He evolved an expression which is called Reynolds Number and is commonly abbreviated Re.

Hence, the flow around a circular cylinder is expressed by Reynolds in dimensionless form as:

$$Re = \frac{VD}{\nu} \qquad (3.1)$$

Reynolds found experimentally a value which is called the Critical Reynolds Number. For values of Re less than the critical, the flow was smooth or laminar; for values greater than the critical Re, the flow was turbulent.

At very low Reynolds numbers ($Re<5$) the flow about a circular cylinder follows Stoke's law, [34] where the flow is laminar and the streamlines close behind the cylinder (figure 3.1(a)).

As the flow increases the streamlines widen and at approximately $Re = 5$ or 6 the flow separates from the rear of the cylinder and a pair of attached vortices form as illustrated in Figure 3.2(b).

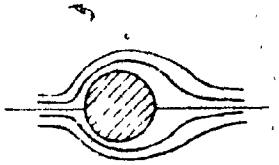

(a) $Re < 5$

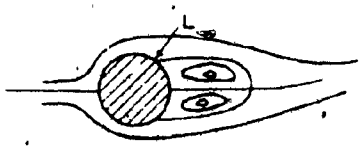

(b) $5 < Re < 30$

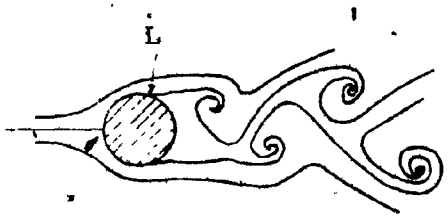

(c) $30 < Re < 150$

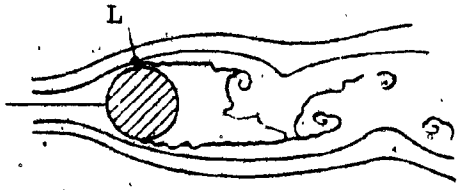

(d) $150 < Re < 10^5$

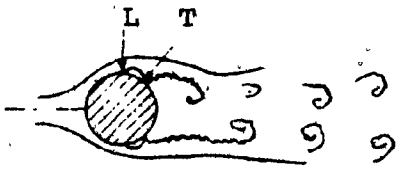

(e) $10^5 < Re < 3 \times 10^6$

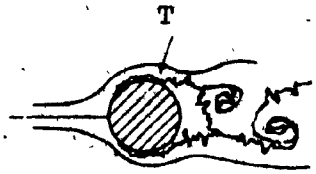

(f) $3 \times 10^6 < Re$

L — Laminar flow separation

T — Turbulent flow separation

Figure 3.1 The Flow Development Around an Infinitely Long Circular Cylinder with Increasing Reynolds Number.

These vortices, it was shown by Föppl [35]could maintain a symmetric equilibrium position for only these low values of Re.

As Reynold's number increases the vortices become elongated in the streamwise direction and the laminar wake becomes more unstable. At a Reynolds number of about 30 to 40 the instability of the wake leads to the development of a "vortex street" (figure 3.1(c))with vortices being shed alternately from either side of the cylinder at a periodic rate which increases with increasing Re.

In all these cases (i.e Re < 40) approximate solutions of the Navier - Stokes equations appear to represent the observed flow phenomena well.

Between Re=150 and about 10^5 (the subcritical regime) the vortex shedding becomes less regular and turbulence in the wake spreads progressively upstream towards the cylinder. Separation of the laminar boundary layer on the cylinder moves progressively forward with increasing Re until Re reaches a value of the order 10^5 when separation occurs on the forward part of the cylinder at a value of θ between about 70° and 80° figure 3.1(d).

As the Reynolds number increases above a value of about 10^5 transition from laminar to turbulent flow in the boundary layer moves along the rear of the cylinder. The Reynolds number at which this actually occurs depends strongly on the free-stream turbulence level and surface roughness - the greater the turbulence level and surface roughness the lower will this value be. The laminar boundary layer separates initially

at about $\theta = 90°$ to $100°$ just ahead of the transition point to turbulent flow, but because the turbulent boundary layer can withstand a greater adverse pressure gradient, the boundary layer reattaches just downstream of where transition occurs to form a localized separation bubble.

Turbulent re-separation occurs further back on the cylinder at about $\theta = 120° - 140°$ as shown in figure 3.1(e).

This rapid rearward movement of the final separation point over a small range of Re results in a higher base pressure and hence a rapid drop in the drag coefficient from about 1.2 to 0.27 for a smooth cylinder.

As Re further increases, transition to turbulent flow occurs further forward on the cylinder with a subsequent increase in boundary layer thickness over the rear of the cylinder and a resulting shift forward of the rear turbulent separation point.

The laminar separation bubble progressively shrinks in size until at a Reynolds number of about 3×10^6 transition occurs at the point where the laminar boundary layer would otherwise have separated ($\theta = 90°$) and the bubble disappears. The forward movement on the rear of the cylinder of the turbulent separation point is accompanied by a re-widening of the wake, a lower base pressure and a subsequent increase in Drag Coefficient (C_D) from about 0.27 to about 0.55 for a smooth cylinder.

At Reynolds numbers higher than about 5×10^6 the transition point moves onto the forward face of the cylinder; the turbulent separation point remains on the rear of the cylinder and its forward movement becomes less sensitive to further

increases in Re.

Periodic vortex shedding continues and C_D reaches a maximum value.

At even higher Reynolds numbers, above about 10^7 in a flow of low turbulence for a smooth cylinder, the flow around the cylinder becomes almost entirely turbulent. With the transition point fixed, further increase in Re serves only to reduce the boundary layer thickness and hence the skin friction coefficient. Thus the pressure distribution becomes largely independent of Re and the drag coefficient varies slowly with increasing Re.

The existence of vortex shedding and periodic wakes in flow about a cylinder has been known for a long time. This fact is documented by Leonardo da Vinci's art work where he illustrates in sketches the formation of alternate vortices and periodic wakes past a cylinder in uniform flow.

Experimental work on the determination of vortices and their effects was first carried out by V. Strouhal in 1882 who developed a non dimensional term, similar to that of Reynolds, to determine the frequency at which the vortices are shed. This term named after Strouhal is given by:-

$$S = \frac{fD}{V} \qquad (3.2)$$

Where f is the rate at which the vortices are shed

D is the diameter of the cylinder

V is the flow velocity

Later, in 1908, Benard and Von Karman related in their work the periodicity of the vortex shedding to a "vortex street" wake. Von Karman in his work "Mechanism of Drag" showed that the wake was unstable unless the vortices arranged themselves in two parallel rows with equal spacing and with the center of the vortices of one row opposite the midpoint between two vortices of the other row. He also determined that the spacing ratio, b/a, must equal 0.281, where a is the longitudinal spacing and b the lateral.

A great deal of work followed, intended mainly in confirming Von Karman's results. Hence some of the most notable work was done by Birkhoff [36] , Tritton [37] , Humphreys [38] and Roshko [39] only to mention a few.

The "Vortex street" as described above moves accordingly up and down and the flow pattern as illustrated in Figure (3.1(c) comes into existence. The oscillations are the physical source of the tones in an "Aeolian Harp" produced by wind (Aeolus was the Greek God of the wind). The whole system of the vortex street moves in the same direction as the body, with the velocity w, measured against the resting fluid. Based upon the length "a" of the "street" (Figure 3.2) the drag coefficient is:

$$C_D = 1.6 \frac{w}{V} - 0.64 \left(\frac{w}{V} \right)^2 \qquad (3.3)$$

Where V is the velocity of the cylinder. Unfortunately neither the relative velocity w nor the dimension 'a' can be predicted by theory.

The number of vortices formed at one side of the street in the unit time is:

$$f = (V - w) / a \qquad (3.4)$$

Where (V-w) is the velocity of the cylinder moving away from a system fixed to the cores.

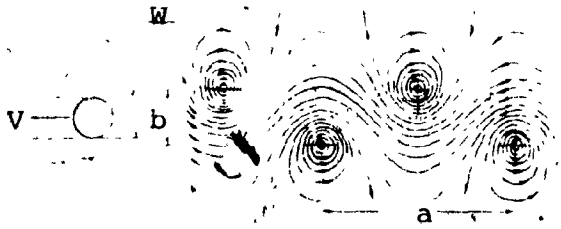

Figure 3.2 Theoretical pattern of the Vortex Street.

Summarizing the above, the "vortex street" may begin at a Reynolds number as low as [40] and persist up to about a $Re = 2 \times 10^5$. This region of flow as described earlier is termed the subcritical region.

Experimental tests on a cylinder in supercritical flow (2×10^5 Re 3.5×10^6) where conducted by Roshko [39]. The dominant periodic components which were attributed to vortex shedding were identified with the use of a hot-wire probe. However, vortex shedding could not be found in the transition region. This fact suggests that the vortex shedding pattern breaks down at the critical flow velocity and re-establishes itself in the supercritical region. It is not certain that the vortex shedding pattern in this region of flow is similar in nature to the conventional vortex shedding pattern or whether this periodic component is due to same other form of periodicity in the wake.

Here, it is worth mentioning the influence of surface roughness in the flow.

Increasing surface roughness has the effect of increasing the boundary layer thickness over the cylinder and of causing transition to turbulent flow on the rear of the cylinder to occur at considerably lower Reynolds numbers. The resulting effect of this condition is the rapid fall in drag coefficient to occur at lower Reynolds numbers than for a smooth cylinder in the same free stream. An important factor to be borne in mind in calculating fluid dynamic forces at the design stage is that the growth of localized regions of roughness particles on an otherwise smooth cylinder (such as ice particles on guy wires, rust etc.) can have a very significant effect on the forces and pressures on the smooth cylinder.

In particular, considerable lift forces, of the same order as the drag force, can be generated if the roughness growth occurs near the transition point so as to cause the shift in the separation point on one side of the cylinder to be very different from that on the other side as the Reynolds number increases through the critical range. Similar lift forces are generated on stranded cables inclined to the free-stream direction causing a similar differential movement of the separation point to occur on upper and lower surfaces at Reynolds number near the critical value.

3.2 The Nature of the Fluctuating Forces Induced by Vortex Shedding

Vortex shedding due to wind action induces fluctuating dynamic forces in stacks.

There are three forms of dynamic action as follows:

(i) Accross - flow oscillation

(ii) in flow oscillation

(iii) Ovalling oscillation

Fortunately, oscillations (ii) and (iii) are small and in most cases may be ignored.

(i) Accross flow or lateral oscillations are by far the most important in that, if they are not properly considered they may lead into the destruction of the structure.

It is well known that alternating vortex shedding induces regions of low pressure. This in turn results in a net "lift force", normal to the wind flow, alternating in direction as vortices are shed, and a force parallel to the flow termed as "drag force" which fluctuates in magnitude. The vortex shedding may either be periodic, that is at a constant frequency of shedding (fvs) and amplitude, or ramdom. This of course depends greatly on the turbulence properties of flow and the appropriate Reynolds number.

It has been demonstrated experimentally by Von Karman that a "street" of alternate vortices forms a stable system, if properly arranged, in accordance with the following expression:

$$\frac{b}{a} = \frac{1}{\pi} \cosh^{-1} \sqrt{2} = 0.281 \qquad (3.5)$$

In fact, Von Karman indicated experimentally that the width of the "vortex street" b, is 1.2D, in cylindrical bodies, with the spacing of the vortices at 4.3D and relative velocity of V-W=0.14V as shown in Figure 3.2.

For a circular cross-section of a cylinder the frequency of vortex shedding may be expressed in non-dimensional form by the Strouhal number for this case as:

$$S = \frac{V - 0.14V}{4.3D} = \frac{0.2V}{D} \qquad (3.6)$$

From this equation it could be seen that the Strouhal number is dependent upon the Reynolds number which is not the case in cross sections with sharp edges such as squares and triangles. In these cases the flow separation points are very well fixed by the position of the edges and therefore the pattern does not change with Reynolds number.

Tall stacks with generally low damping are very responsive to the oscillating forces and oscillation starts as the wind velocity approaches the critical value at which the vortex shedding frequency equals the natural frequency.

In most steel stacks only the first mode of oscillation need be considered as it generates maximum amplitudes. However, in stacks with high degree of taper and small tip diameer, higher modes should also be investigated. This is mainly due to the fact that the natural frequency is changing, with height and the variation in the cross section. This consideration was taken into account at the design stage

of the Browns Ferry Nuclear Power Plant chimney at Alabama. [40] which has a height of 600 ft and a tip diameter of 6 ft, and was designed for vortex shedding at frequencies corresponding to the first, second and third modes.

At lower amplitudes of oscillation, approximately in the order of 1 to 2% of the stack diameter, the frequency and hence the response of the wind induced fluctuating forces is random in nature with a major portion of the generated energy distributed over a narrow range of frequencies close to frequency of shedding.

At amplitudes of oscilation of more than 2% of the stack diameter, the local forces are amplified due to vortex shedding. These fluctuating forces and their response are then nearly periodic resulting in more or less constant amplitude response at the natural frequency and they may be described in terms of a fluctuating lift coefficient.

The lift coefficient varies sinusoidally with time at the frequency of the vortex shedding. The fluctuating force per unit height at any given height Z of the stack is given by:

$$F(Z) = \tfrac{1}{2} C_L \; V_c^2 D(Z) \sin t \qquad (3.7)$$

where C_L is the peak dynamic lift coefficient.

In general, C_L reduces as Reynolds number increases and increases with increasing oscillatory movement. It has been estimated both experimentally and theoretically that the value of C_L varies from 0.15 to 1.3. This is not necessarily true in actual structures due to variations in surface and wind

conditions.

A rather conservative value of 0.66 has been suggested by Maugh and Rumman [41] for design purposes.

An extensive study carried by P. Sacks, [42] based on both wind tunnel tests and oscillations on full-sized stacks indicated values of C_L between 0.20 to 0.33 in the wind tunnel and C_L between 0.12 to :19 in four full sized lined and unlined steel, rivetted and welded stacks.

(ii) In-Flow Oscillation is caused by two mechanisms, either by the oscillating drag force or by the simultaneous vortex shedding.

Associated with alternate vortex shedding is a fluctuating drag force capable of inducing oscillations in the direction of the mean flow. This excitation reaches maximum value at around one-half of the critical wind speed for accross flow oscillations.

Simultaneous vortex shedding from each side of the cylindrical structure causes a fluctuating drag force which may induce significant in line oscillations. This excitation reaches maximum value at Strouhal numbers in the range of 0.45 to 1.0.

Generally, in-wind oscillations are very weak and easily damped out thus not creating any severe conditions of aerodynamic instability.

(iii) Ovalling Oscillations, another mechanism of wind excited oscillations, is found mainly in thin shelled steel stacks, it involves mainly circumferentional deflections of the cylinder wall like an elastic ring or shell. This

is due to the fact that the pressure distribution around a section varies periodically. This can lead to periodic distortion of an unstiffened thin-walled cross section such as a large diameter steel stack and is termed "ovalling" or "breathing". The effects of ovalling in most cases are not worth considering except in the cases where large diameter thin-walled cross sections are used.

Finally, it should be emphasized that although the above described mechanisms of aerodynamic instability have been fully investigated, the prediction of the performance of a proposed steel stack may not be always possible. This is mainly due to the fact that model tests do not allow for the random variation of wind speed and direction that occur in nature. Also they do not represent accurately the disturbance of the air flow pattern around the chimney.

Rather than predicting the performance of a proposed steel stack it is quite logical to investigate means of avoiding the dynamic wind problems. It is the intension of this study to examine possible ways of treating effectively these vibration mechanisms as described.

CHAPTER 4

DYNAMIC RESPONSE OF STEEL STACKS

4.1 SELF SUPPORTED STEEL STACKS

For dynamic analysis, a self supported steel stack may be idealized as a Lumped-mass simple system shown in Figure 4.1

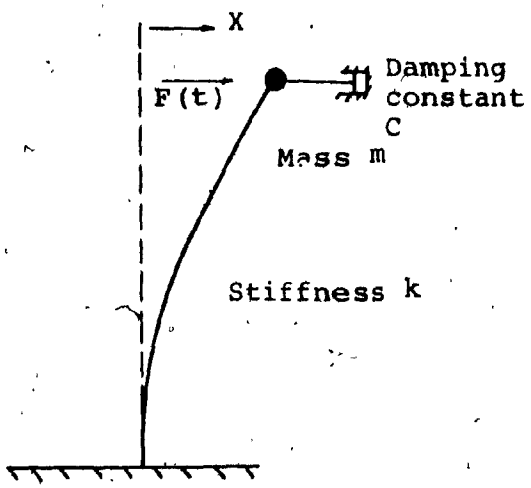

Figure 4.1

The system is constrained to move only along the X-direction and it consists of a single mass m, supported by a light cantilever with a linear stiffness k, and interal damping constant C.

The wind loading is represented by the force F(t) applied to the mass and is time dependent.

At some time t (where $t > 0$) from theoretical mechanics it is known that: Force = mass x acceleration.

This equation may be applied in the system as follows:

$$F(t) - kx - c\dot{x} = m\ddot{x} \qquad (4.1)$$

or by rearranging the terms:

$$m\ddot{x} + c\dot{x} + kx = F(t) \qquad (4.2)$$

There the term $m\ddot{x}$ is called the inertia force. The solution of Equation (4.2) is obtained by setting $F(t) = 0$ and is composed of a complementary function and a particular integral which is dependent upon the form of $F(t)$.

The complementary function is the solution of the damped free vibration equation which in fact yields a number of useful parameters.

Assuming that the motion can be expressed as:

$$x = xoe^{\lambda t} \qquad (4.3)$$

Equation (4.2) by setting $F(t) = 0$ can be expressed as

$$(\lambda^2 m+\lambda c+k)x=0 \qquad (4.4)$$

The solution of Equation (4.4)

$$x = 0$$

or since x is not always zero,

$$\lambda^2 m+\lambda c+k=0 \qquad (4.5)$$

The solution of Equation (4.5) is:

$$\lambda = -\frac{c}{2m} \pm \sqrt{(\frac{c}{2m})^2-\frac{k}{m}} \qquad (4.6)$$

Substituting Equation (4.6) into Equation (4.3)

$$x=x_o \exp[-\frac{ct}{2m}]\exp\left[i\sqrt{\frac{k}{m}-(\frac{c}{2m})^2}\right]t \qquad (4.7)$$

For positive values of c the first exponential in Equation (4.7) is afunction which decreases with time (decays).

The second exponential in the same equation decreases only if:

$$\frac{k}{m} < \left(\frac{c}{2m}\right)^2$$

However if $\frac{k}{m} > \left(\frac{c}{2m}\right)^2$, the second exponential oscillates as a function of time.

The net result from Equation (4.7) is a decaying oscillation as shown in Figure 4.2.

The period of oscillation is given by:

$$T = \frac{2\pi}{\frac{k}{m} - \left(\frac{c}{2m}\right)^2} \qquad (4.8)$$

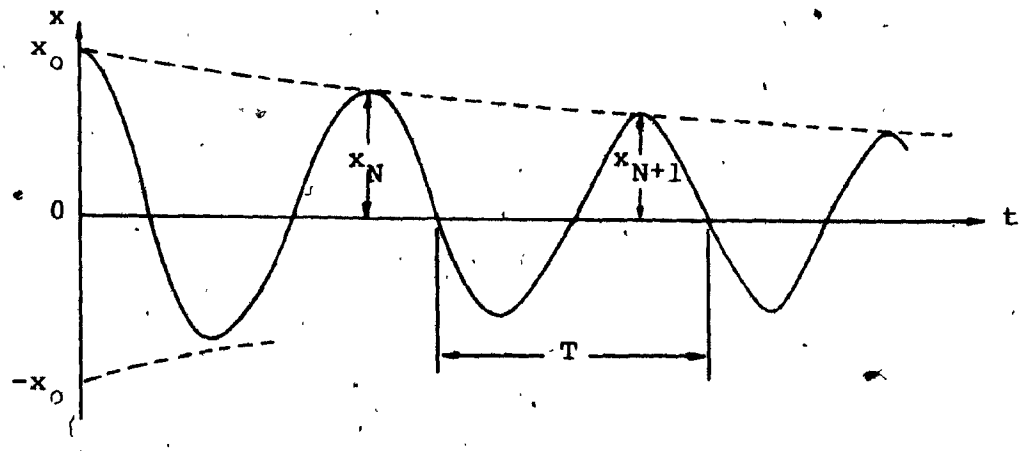

Figure 4.2 Positively damped free vibration.

The coresponding frequency of oscillation which is the inverse of the period or $\frac{2\pi}{T}$ rad/s is:

$$f_d = \frac{1}{2\pi}\sqrt{\frac{k}{m} - \left(\frac{c}{2m}\right)^2} \quad \text{Hz}$$

or

$$\omega_d = \sqrt{\frac{k}{m} - \left(\frac{c}{2m}\right)^2} \quad \text{rad/s} \qquad (4.9)$$

This frequency is the damped natural frequency of the system.

If the internal damping constant c is zero then the undamped natural frequency is derived from Equation (4.9) as:

$$f_n = \frac{1}{2\pi}\sqrt{\frac{k}{m}} \quad \text{Hz}$$

or

$$\omega_n = \sqrt{\frac{k}{m}} \quad \text{rad/sec} \qquad (4.10)$$

In the absence of damping, the amplitude of oscillation is constant as shown in Figure 4.3.

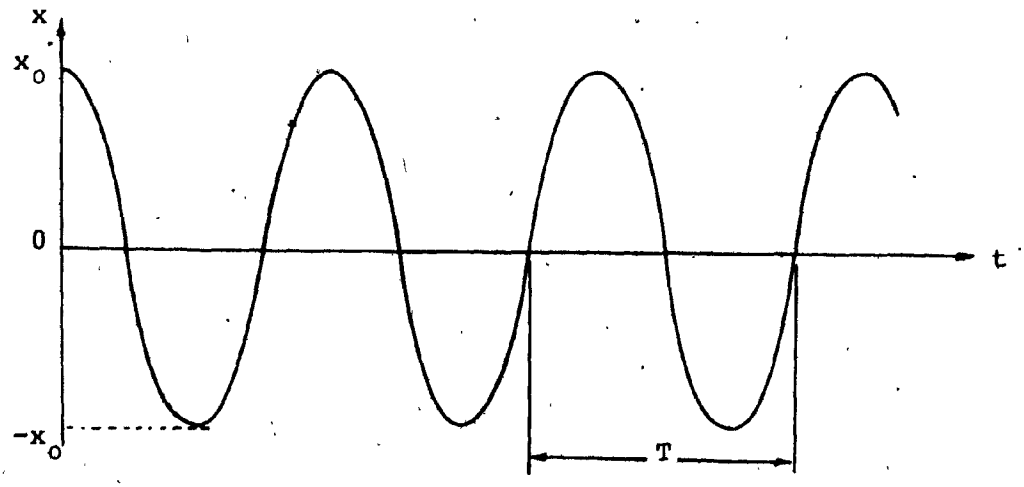

Figure 4.3 Undamped free vibration.

However if c is negative, the first exponential in Equation (4.7) becomes an increasing function with time and the second exponential becomes $\frac{k}{m} > (\frac{c}{2m})^2$ with the net result of diverging oscillation as shown in Figure 4.4.

In case where the square root term in Equation (4.6) is zero, the required damping necessary for the system to come to rest

without oscillation is called the critical damping and is given by:

$$c_{crit} = 2\ km \qquad (4.11)$$

In order to relate the damping of a structure to this critical value, a new term has been introduced known as damping ratio (ζ).

$$\zeta = \frac{c}{2\ km} \qquad (4.12)$$

This parameter is characteristic of a structure depending mainly on material properties and geometry.

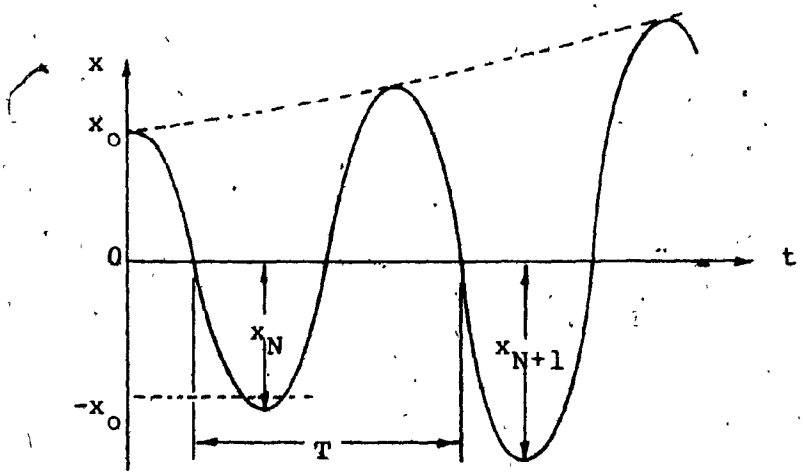

Figure 4.4 Negatively damped free vibration.

The following are typical values of damping for some selected structures.

Structure	Typical range of ζ
Bridges, steel	0.003-0.01
Bridges, reinforced concrete	0.005-0.02
Stacks, concrete	0.005-0.15
Stacks, steel	0.003-0.010
Towers, steel latice	0.003-0.013

Substituting Equation (4.12) and (4.10) into Equation (4.6)

$$\lambda=-\omega_n\zeta\pm i\omega_n\sqrt{1-\zeta^2}$$

From this Equation, Equation (4.7) becomes:

$$x=x_0\exp(-\omega_n\zeta t)\exp(i\omega_n\sqrt{1-\zeta^2}t) = x_0\exp(-\omega_n\zeta t)\exp(i\omega_d t) \quad (4.14)$$

From Figures 4.2 and 4.4 another useful damping measure can be defined from the ratio of the amplitudes x_N and x_{N+1}, the logarithmic decrement, (δ) defined by:

$$\delta = \log_e\frac{x_N}{x_{N+1}} = \frac{2\pi\zeta}{\sqrt{1-\zeta^2}} \quad (4.15)$$

For steel stacks where ζ is of the order of 0.003 - 0.010,

$\sqrt{1-\zeta^2}=1$

Hence, $\delta=2\pi\zeta$ and $\omega_d=\omega_n$

The particular integral part of the solution of Equation (4.2), is the response to the forcing function F(t).

This F(t) function can simply be expressed as a summation of periodic functions of similar responce characteristics.

Therefore, expressing F(t) as $F(t)=F_0e^{i\omega t}$ and x as $x=x_0e^{i\omega t}$ Equation (4.2) becomes:

$$(-\omega^2m+i\omega c+k)x_0=F_0 \quad (4.16)$$

The particular integral solution of this equation is:

$$F_0e^{i\omega t} = x(k-\omega^2m+i\omega c)$$

or

$$F_0e^{i\omega t} = mx\left(\frac{k}{m}-\omega^2+i\frac{c}{m}\omega\right)$$

or

$$x = \frac{F_0 e^{i\omega t}}{m\left(\frac{k}{m} - \omega^2 + i\frac{c}{m}\omega\right)} \quad \frac{F_0 e^{i\omega t}}{k\left[1 - \left(\frac{\omega}{\omega_n}\right)^2 + i2\zeta\frac{\omega}{\omega_n}\right]} \qquad (4.17)$$

The term $\frac{1}{\left[1 - \left(\frac{\omega}{\omega_n}\right)^2 + i2\zeta\frac{\omega}{\omega_n}\right]}$ is termed as the Mechanical Admittance and is denoted by $|H(\omega)|$ and is written as:

$$|H(\omega)| = \frac{1}{\left[1 - \left(\frac{\omega}{\omega_n}\right)^2\right]^2 + \left[2\zeta\frac{\omega}{\omega_n}\right]^2} \qquad (4.18)$$

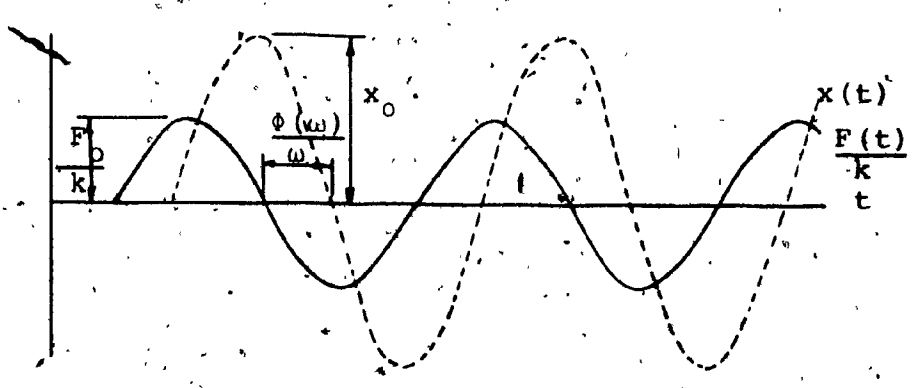

Figure 4.5

This parameter measures the magnification of the static deflection, $\frac{F_0}{k}$ resulting from the application of F_0 as a dynamic loading. Another important parameter in defining the relationship between the input force F and the resulting deflection x is the phase angle of $H(\omega)$ or argument, given as

$$\phi(\omega) = \tan^{-1}\left[\frac{2\zeta\frac{\omega}{\omega_n}}{1 - \left(\frac{\omega}{\omega_n}\right)^2}\right] \qquad (4.19)$$

In terms of mechanical admittance and phase angle, Equation (4.17) can be written as:

$$x = \frac{F_0}{k}|H(\omega)|e^{i[\omega t - \phi(\omega)]} \qquad (4.20)$$

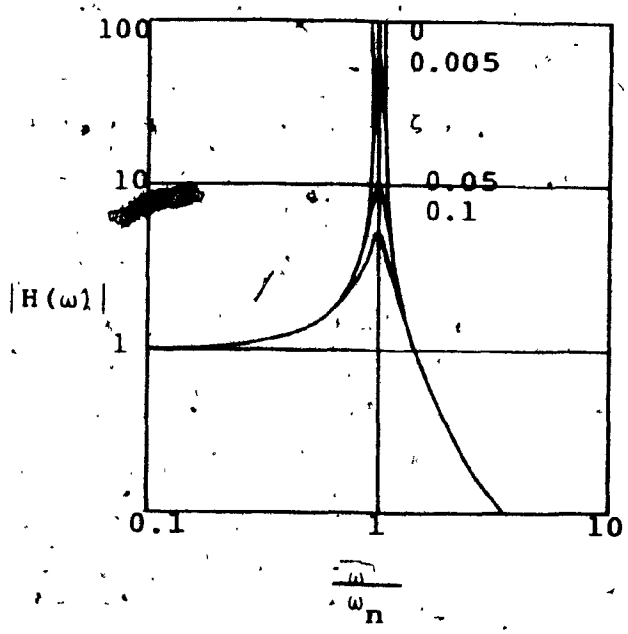

Figure 4.6 Magnitude of admittance function

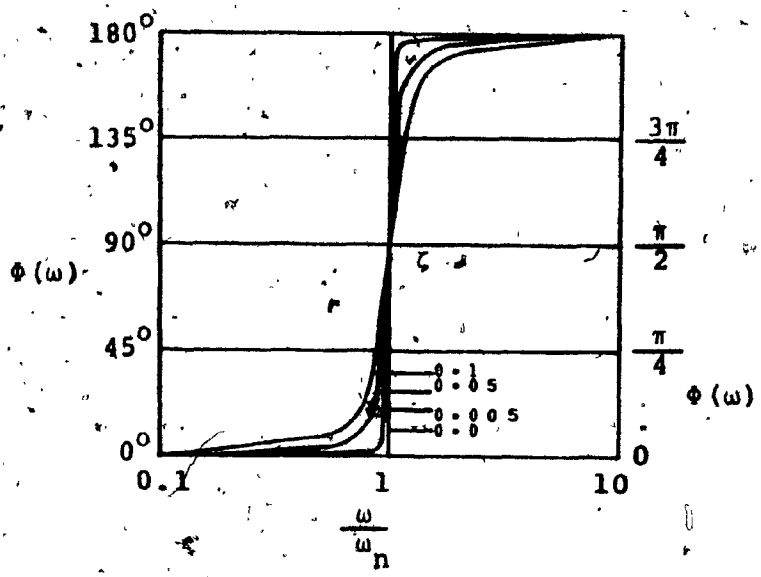

Figure 4.7 Phase angle of admittance function.

This equation may be represented graphically by Figure 4.5. The relationship of the variation of $|H(\omega)|$ with frequency ratio $\frac{\omega}{\omega_n}$ and damping ratio ζ is illustrated in Figure 4.6. It could be seen that the magnitude of admittance function reaches a maximum when $\frac{\omega}{\omega_d} = 1$ which is called the Resonant condition. For small values of $\frac{\omega}{\omega_d}$ the response is governed by the stiffness k and maximum deflection is approximately the same as the static value whereas for large values of $\frac{\omega}{\omega_d}$ the response is governed by the mass m and maximum deflection is less than the equivalent static value. The response in the region near $\frac{\omega}{\omega_d} = 1$ is controlled by the damping and the maximum deflection may be much larger than the equivalent static value. Figure 4.7 illustrates the variation of the phase angle $\phi(\omega)$ with frequency and damping ratio.

Finally, if F(t) is a random function of time then a function giving the frequency distribution of statistical properties of fluctuating wind can be introduced in equivalent form of Equation (4.20). This function known as Spectral density function of F(t) is given as:

$$S_{xx}(\omega) = \frac{|H(\omega)|^2}{k^2} S_{FF}(\omega) \qquad (4.21)$$

When the function F(t) is acting over a range of frequencies, it is necessary to derive a mean square value of the random response. This of course, could be calculated by integrating Equation (4.21) as follows:

$$\sigma^2(x) = \int_0^\infty S_{xx}(\omega)\,d\omega = \int_{-\infty}^{\infty} \omega S_{xx}(\omega)\,d[\log_e \omega] \qquad (4.22)$$

Summarizing all the above, the complete solution of Equation (4.2) for a periodic function F(t) is the sum of the free vibration response as written in Equation (4.14) and the forcing function response from Equation (4.20) with parallel consideration of the phase angle $\Phi(\omega)$.

Hence:

$$x=x_0\exp(-\omega_n\zeta t)\exp(i\omega_n\sqrt{1-\zeta^2}t)+\frac{F_0}{k}|H(\omega)|\exp(i[\omega t-\Phi(\omega)]) \qquad (4.23)$$

Note that for a random forcing function, Equation (4.20) is replaced by Equation (4.22) in Equation (4.23).

The forcing vibration response of a self supported steel stack will always be at the frequency of the forcing function in steady state forced vibration, whereas the free vibration part of the response is at the damped natural frequencies of the stack.

4.2 GUYED STEEL STACKS

It has been shown that the amplitude of lateral oscillations of self suported steel stacks is dependent upon the structural stiffness (k) and damping ratio (ζ) parameters.

Since, these parameters exhibit considerably low values in tall stacks, a widely accepted method in increasing their values is by the use of guy cables. In addition, guy cables seem to be cost effective in terms of reduced size of both, the main structure(shell) and foundations.

However, although guy wires may not eliminate oscillations completely, they may introduce new problems through oscillations of the cables themshelves, hence their behaviour and effects on the main structure should be examined.

A guyed stack is subjected to the following loads as shown in Figure 4.8.

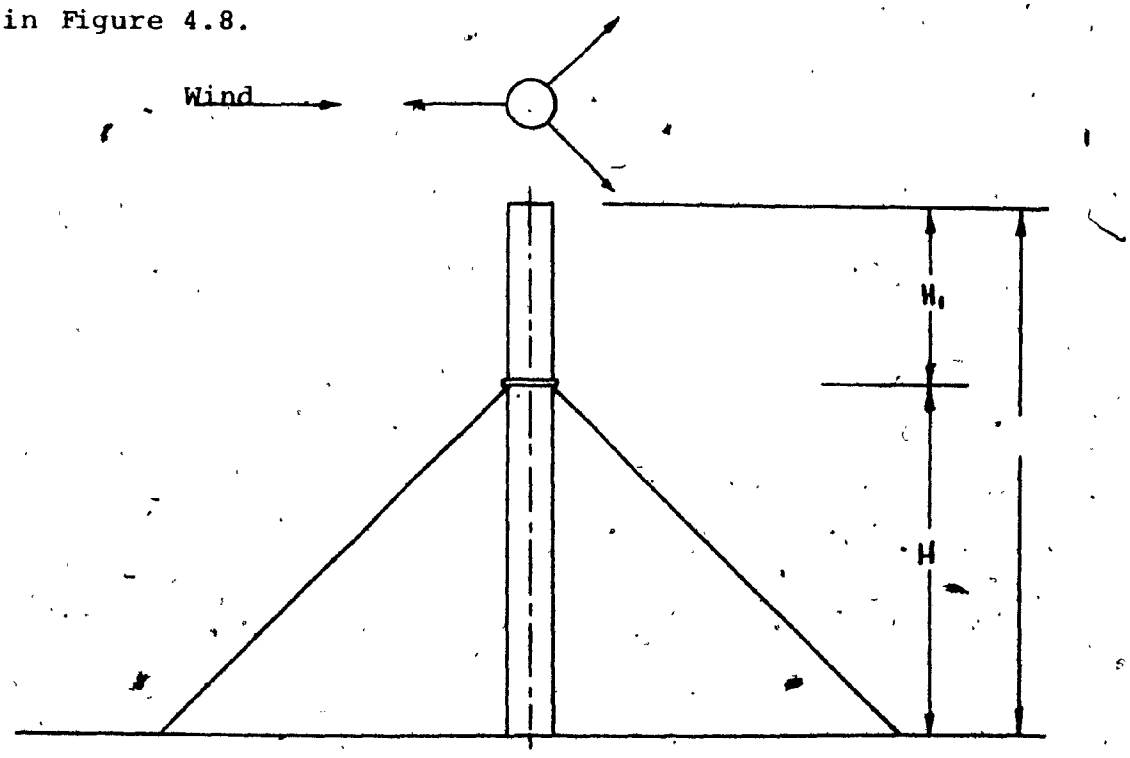

Figure 4.8: Forces acting on a typical guyed stack.

a) Vertical load due to deadweight of the structure and the loads of the supported parts.

b) Vertical and horizontal components due to the dead-weight and erection tension of the guy cables.

c) The vertical and horizontal components of the increase of the guy tensions due to the horizontal wind loads.

Although, the loading conditions on a guyed stack are well defined, analysis of this type of a structure is somewhat complicated due to the nonlinear characteristics it exhibits. Hence, the development of the nonlinear force - displacement relations as well as the correct solution to the nonlinear equations which govern the behaviour of the entire structure, becomes a very difficult task.

The nonlinear characteristics of guyed stacks originate from several factors the most important of which are:

-The variation of the effective flexural stiffness resulting from increasing axial load.

-The displacement of the upper ends of the guy cables resulting from contraction of the shell structure caused by flexure and compression.

-The variation of wind load on the guys.

Since guy cables are responsible for a major portion of the main structure's axial loads, it is useful to have accurate and reliable static and dynamic analysis in order to relate the variables associated with guy cables, such as the change in cable tension as a function of the stack movement.

Statically, a guy cable, under the influence of gravity loading alone, hangs in a shape of an arc of a catenary. Figure 4.9, illustrates the forces acting on a typical guy.

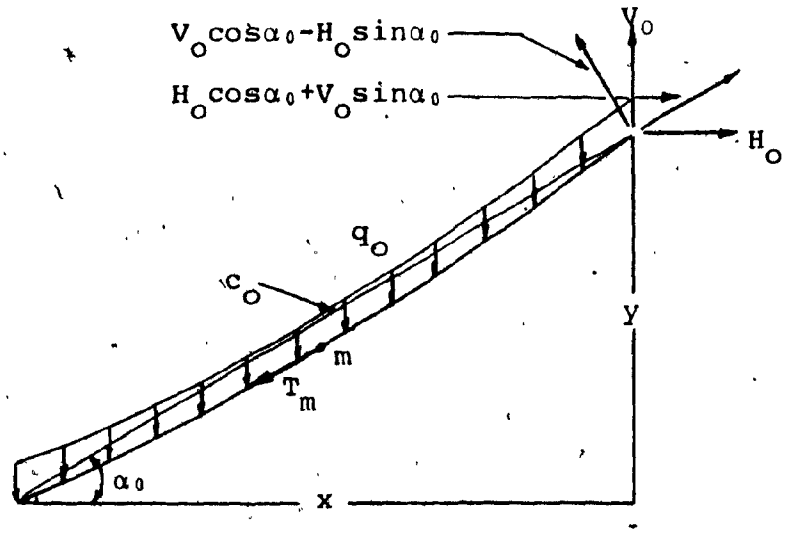

Figure 4.9: Cable geometry under gravity load only.

The arc length L_o, under the influence of gravity load alone, is given by:

$$L_o = \left[\frac{4H_o^2}{q_o^2}\sinh^2\left(\frac{q_o c_o \cos\alpha_o}{2H_o}\right) + c_o^2\sin^2\alpha_o\right]^{\frac{1}{2}} \qquad (4.24)$$

where: H_o = Horizontal component of the reaction at the upper end of the guy.

q_o = Gravity load per unit length.

α_o = Angle between chord and horizontal.

c_o = Chord length.

Taking the sum of the moments about the base of the cable in Figure 4.9, it is seen that:

$$V_o x = H_o y + \frac{q_o c_o x}{2} \quad \text{or} \quad V_o = H_o\left(\frac{y}{x}\right) + \frac{q_o c_o}{2} \qquad (4.25)$$

Since $(\frac{y}{x}) = \tan\alpha_o$, Equation (4.25) may be rewritten as:

$$V_o = H_o \tan\alpha_o + \frac{q_o c_o}{2} \qquad (4.26)$$

For any given guy cable, the values of q_o, α_o, c_o, and H_o are specified and L_o and V_o may be determined from Equations (4.24) and (4.26) respectively.

In determining the equations of motion for a guy cable under forced vibration due to wind action, it is proposed to determine the variations in horizontal force exerted on the structure when the support point is executing harmonic motion.

Assuming that the wind force on the guy is constant over the length of the cable and that the plane and curvature of its catenary have been altered due to wind loading, Equation (4.24) is then changed to:

$$L = [\frac{4H^2}{q} \sinh^2(\frac{qc\cos\alpha}{2H}) + c^2\sin^2\alpha]^{\frac{1}{2}} \qquad (4.27)$$

and Equation (4.26) becomes:

$$V = H \tan\alpha + \frac{qc}{2} \qquad (4.28)$$

where: q = The vector sum of q_o and wind load W, per unit length of cable

H = The component of the reaction of the upper extermity of the guy which is no longer horizontal but is perpenticular to q and lies in the new plan of the catenary.

c = The variable chord length.

V = The reaction at the upper extremity of the cable that is parallel to the load q and lies in the

new plane of the catenary.

α = The angle between a plane normal to the guy cable and the direction of q.

The variables α and q of Equations (4.27) and (4.28) as well as the angle between the initial and new planes of the catenary β as shown in Figure 4.10, are completely determined by the initial state of the guy and the magnitude and direction of the velocity of the wind on the cable.

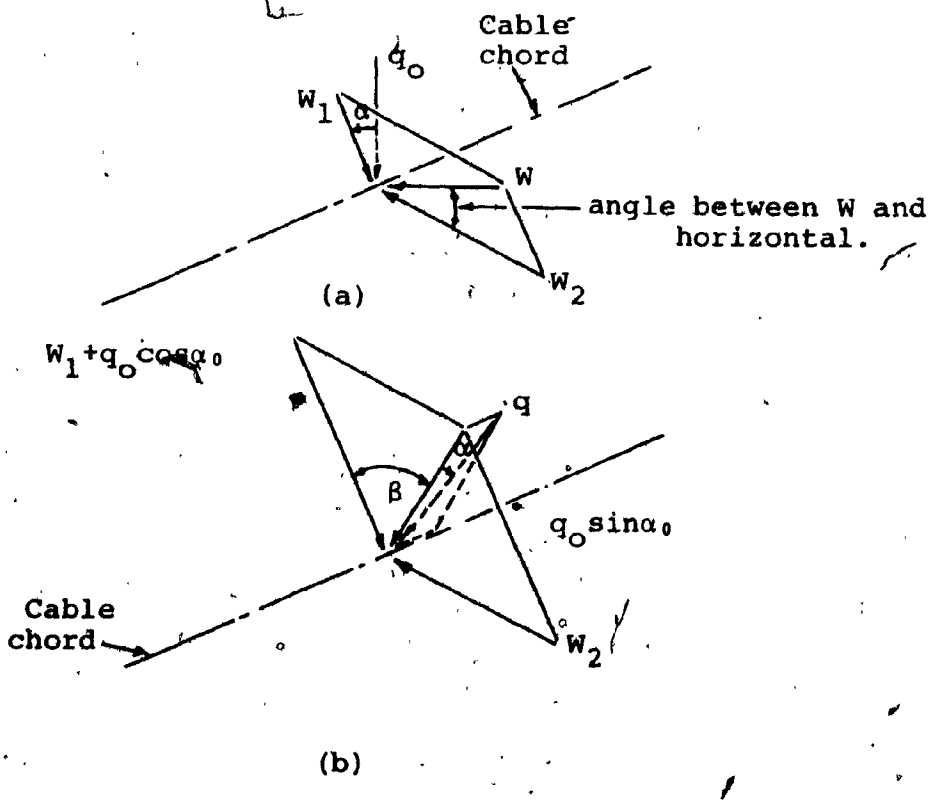

Figure 4.10: Components of wind and gravity forces on cable element.

The magnitude and direction of the wind load W, may be determined from aerodynamic considerations. This load may be broken into components as indicated in Figure 4.10(a) and added to the components of the gravity load as shown in Figure 4.10(b).

From Figure 4.10(b), it is evident that the resultant intensity of the distributed load on the cable is:

$$q = (W_1 + W_2 + q_o^2 + 2q_o W_1 \cos\alpha_0)^{\frac{1}{2}} \qquad (4.29)$$

and that its position relative to q_o is given by:

$$\beta = \tan^{-1} \frac{W_2}{W_1 + q_o \cos\alpha_0} \qquad (4.30)$$

and $$\alpha = \tan^{-1} \frac{q_o \sin\alpha_0 \cos\beta}{W_1 + q_o \cos\alpha_0} \qquad (4.31)$$

The directions of guy reactions V and H are given by angles α and β and the magnitudes of these forces may be found from Equations (4.27) and (4.28) for any given chord length c.

It is quite obvious therefore, that these two equations constitute force-displacement relationships for the cable since c is a function of the displacement of the upper end of the cable and V and H are components of the force at the point.

The arc length (L), which also appears as a variable in Equation (4.27) is a non-linear parameter in the dynamic analysis of a guy cable. This arises from the fact that the length of the guy varies with the applied load, both static and dynamic, as well as the temperature changes.

Given the fact that applied wind loading is both unsteady and unpredictable, the dynamic analysis becomes a very difficult task.

Thus, the variable length (L) may be taken as:

$$L = L_o + \Delta L \qquad (4.32)$$

Where ΔL is the change in arc length resulting from a change in guy cable tension. In other words it is the elastic extension or retraction due to the additional tension $(\Delta t)t$ or reduction in the initial tension.

The elongation due to a change of tensile stress, dH is:

$$e = \frac{cdH}{A\,E}\left(1+\frac{16\Delta^2}{3c^2}\right) \qquad (4.33)$$

The change in length for a temperature change, $\Delta t°$ is:

$$e_t = \varepsilon_t c\left(1+\frac{8\Delta^2}{3c^2}\right)\Delta t° \qquad (4.34)$$

where: ε_t = coefficient of thermal expansion.

Δ = cable initial sag

From Figure 4.9, it can be seen that the tension in the cable at point m, where the tangent to the cable is parallel to the closing chord c, is equal to:

$$T_m = H_o \cos\alpha_o + V_o \sin\alpha_o - q_o L_m \sin\alpha_o \qquad (4.35)$$

where L_m = arc length from top of cable to point m.

In similar terms, for a cable under both wind and gravity loads:

$$T_{ml} = H\cos\alpha + V\sin\alpha - qL\sin\alpha \qquad (4.36)$$

Assuming that T_m and T_{ml} are the mean values of the tension in the cable, then:

$$\Delta L = (T_{ml} - T_m) \frac{L}{AE}. \qquad (4.37)$$

or, by substituting Equations (4.35), (4.36), (4.27) and (4.28),

$$\Delta L = \left(\frac{H}{\cos\alpha} - \frac{H_o}{\cos\alpha_o}\right)\frac{L}{AE} \qquad (4.38)$$

Although, statically a guyed steel stack may easily be analyzed as it has been shown, the computation of such dynamic parameters as frequencies and modes of natural vibrations poses many sources of ambiguities.

For instance, the axial force acting on the stack itself contains the vertical component of the cable tension. The static component of the axial force however, reduces he natural frequencies slightly and given the fact that when the guy cable is excited by wind, the vertical component of the cable tension fluctuates thus altering the frequencies of the main structure.

A study [44] was conducted to determine the effect of variation of the tension of the cables, which changes the rigidity of the guys, on the natural frequencies.

The results of the model are plotted in Figure 4.11 where the first eleven natural frequencies are shown along with he rigidity of the cables.

From this figure it is evident that the dependence of the natural frequencies is not too strong and weakens considerably

as the order of natural frequencies increases.

Denoting c_R as the design rigidity of the guys, the mean square value of the random response of a guyed steel stack may be derived from Equation (4.22) as:

$$\sigma^2(x) = \frac{1}{c_R} \int_0^\infty \frac{S_{xx}(\omega)\, d\omega}{\sqrt{[1-(\frac{\omega}{\omega_n})^2]^2+[\frac{\omega}{\omega_n} 2\zeta]^2}} \qquad (4.39)$$

where $\omega_n = \sqrt{\frac{c_R}{m}}$

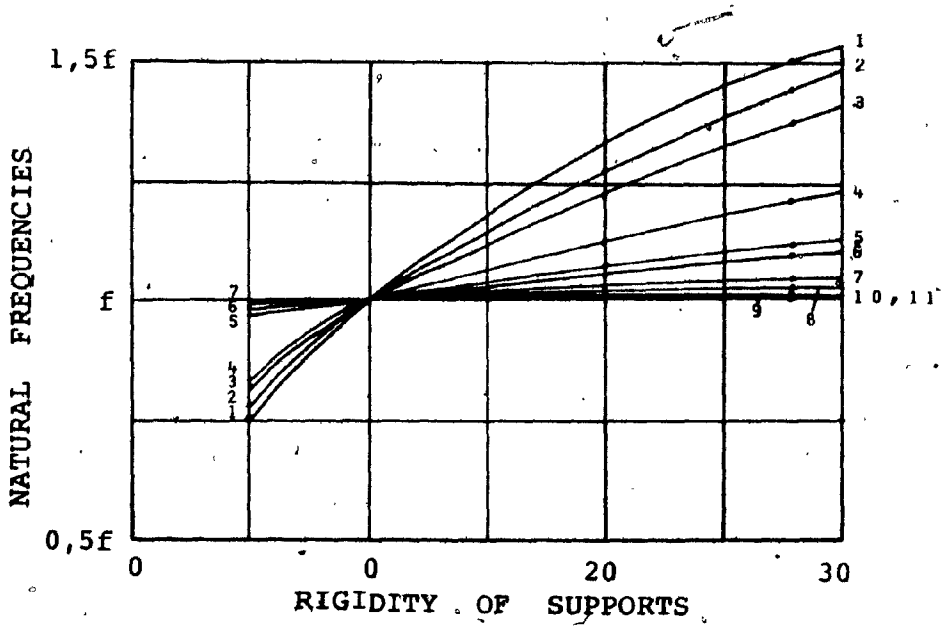

Figure 4.11: Dependence of natural frequencies of stack on rigidity of guy cables.

However, the single most influencial unsteady aerodynamic excitation affecting the guy cables is known as galloping. Galloping, as it is known in the present context, is the

large-amplitude low frequency oscillation of long cylindrical cables in a transverse wind at the natural frequency of the cable.

Even though this type of instability may be taken into consideration at the design stage, potentially dangerous situations may arise on the stability of tall guyed stacks through the accumulation of ice, a very common phenomenon in cold climates such as the Canadian climate. This of course is the result of changing such properties of the cable as cross section, weight, structural stiffness and damping.. These properties along with the angle of attack affect the initial lift and drag coefficients considerably thus creating large amplitude vibrations on the cables and in turn on the supported stack.

If one of the guys supporting a steel stack undergoes galloping oscillation, the amplitude of the motion changes with wind speed but the frequency remains constant and equal to one of the natural frequencies of the system. A theory formulated by Parkinson [45] predicting the response of a stack to the galloping oscillation on the cable, is based on the assumption that the direction of the wind deviates from that normal to the plane of the cable.

Another theory, by Novak [46], indicates that the steady state amplitudes can be estabished if the work done by the input forces of the galloping mechanism along the unstable part of the cable is equal to the work done by the dissipa-

tive forces (structural damping) of the stack in each period of vibration.

Both theories, however, fail to predict the response of iced cables due mainly to the fact that the cross section and the structural properties of iced cables are non-uniform and hence unpredictable.

Apart from these side effects, guy cables seem to be highly beneficial in increasing the structural stiffness and natural frequency of a stack. In addition, since the effect of guy cables is usually non-linear, with stiffness increasing with deflection, they tend to become operative only when some motion occurs and may not eliminate wind-induced oscillations completely.

4.3 THE INFLUENCE OF TAPER

The vortex shedding frequency of a stack in a turbulent shear flow follows the Strouhal Number relationship. This relationship indicates that the frequency of vortex shedding depends on the stack diameter.

In the case of tapered stacks the vortices would be shed at different frequencies along its length and hence resulting in reduced total aerodynamic excitation.

The condition for maximum excitation due to vortex shedding originates from the part of the structure where $Z=Z_c$ and $f_s=f_n$ as shown in Figure 4.12.

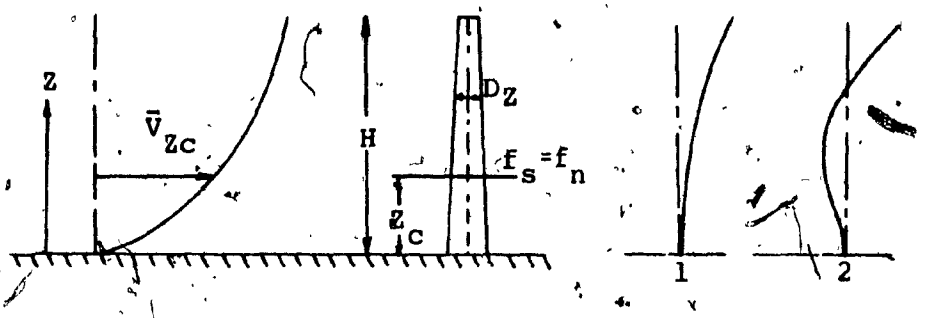

Figure 4.12: Variation of velocity with height along with first two mode shapes of a tapered stack.

The location of the critical cross section where maximum excitation occurs is determined by the local diameter (D_Z) of the structure, the natural frequency (f_n), and the mean wind speed.

Hence, in a tapered stack, as wind speed (V) increases, the location of the critical cross section for the first mode of vibration of the critical cross section for the first

mode of vibration moves down the stack; the lateral oscillation amplitude increases to a maximum, corresponding to a particular value of $\bar{V}$ and then decreases again. For the even higher values of $\bar{V}$, the oscillation amplitude again increases due to excitation of the second mode and in some cases this can be more critical than the response in the first mode.

Experiments on models of tapered stacks [47],[48], indicated however, that the excitation was at least as intense as that of a parallel sided stack of the same efflux diameter as illustrated in Figure 4.13.

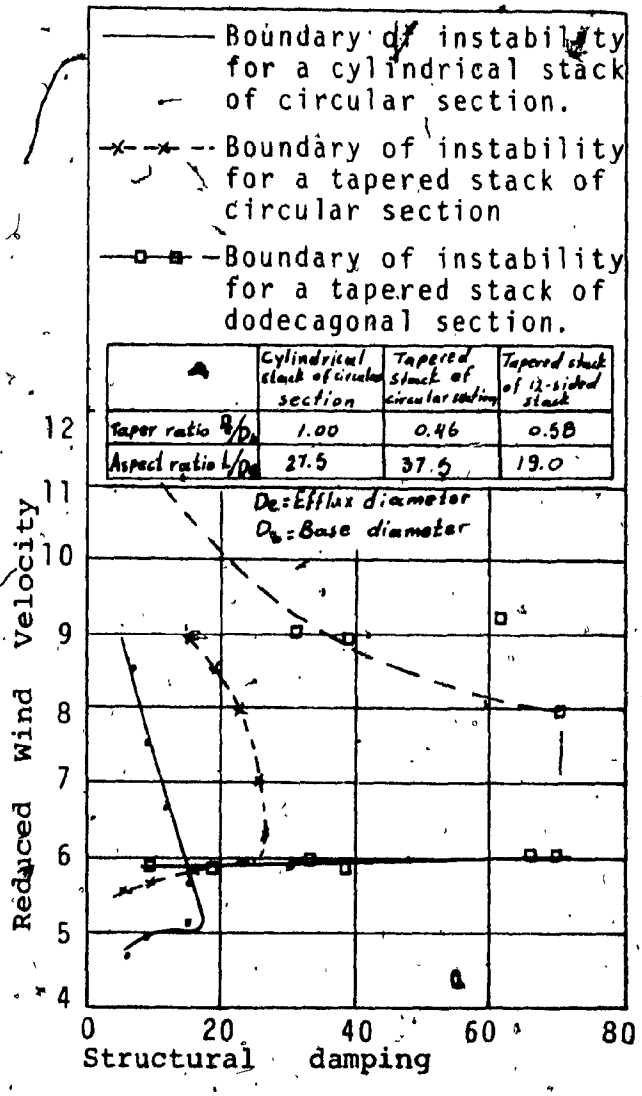

Figure 4.13: Comparison of results for a 12-sided stack with those for cylindrical and tapered of circ. section

The results suggest that the efflux diameter of a stack should be as small as possible, since the critical speed and the aerodynamic excitation, which varies with $\bar{V}^2$, is kept to a minimum, and less structural damping is needed to prevent oscillations.

The influence of taper was confirmed by tests, on a model of a tall tapered stack for the Canada-India reactor project, conducted at National Physical Laboratory, Teddington, England.

The first three modes were excited in the wind tunnel as shown in Figure 4.14. [47]

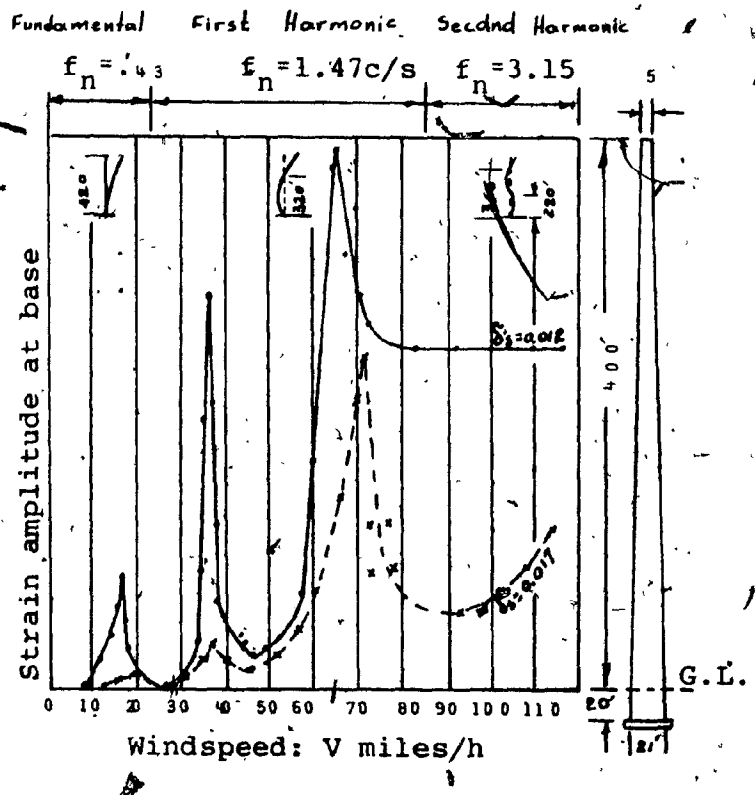

Figure 4.14: Aerodynamic behaviour of a model of a 400 ft high tapered concrete stack.

CHAPTER 5

AERODYNAMIC DEVICES

5.1 PERFORATED CYLINDERS (SHROUDS)

Perforated shrouds were first suggested as a method of preventing oscillations of stacks with circular cross section due to vortex shedding by Price.[15]Since then,further work to refine Price's design and establish the optimum configuration has been carried out by D. Walshe[16].

Although the effectiveness of shrouds is now well proven, including some full-scale results, they have not been used as extensive as other aerodynamic and damping devices.

Interest, however, in perforated shrouds has increased recently mainly due to the advantage they posses over other aerodynamic devices such as strakes in preventing oscillations due to vortex shedding without any considerable increase in drag coefficient.

The work by D. Walshe involved wind tunnel testing of various models of tall stacks in Power Generating Stations.

Wind tunnel studies of a chimney stack for Drax Power Station[43] were conducted at National Physical Laboratory - England, in order to determine the influence of shrouds on the stability of the structure. A linear mode model as shown in Figure 5.1, build to a scale of 1:47, was used in the investigation.

Several shroud configurations were tested to determine the porosity, length and width of the gap between the stack and shroud. Separate tests were conducted for laminar and turbulent wind strams to establish the effects of turbulence on the stack.

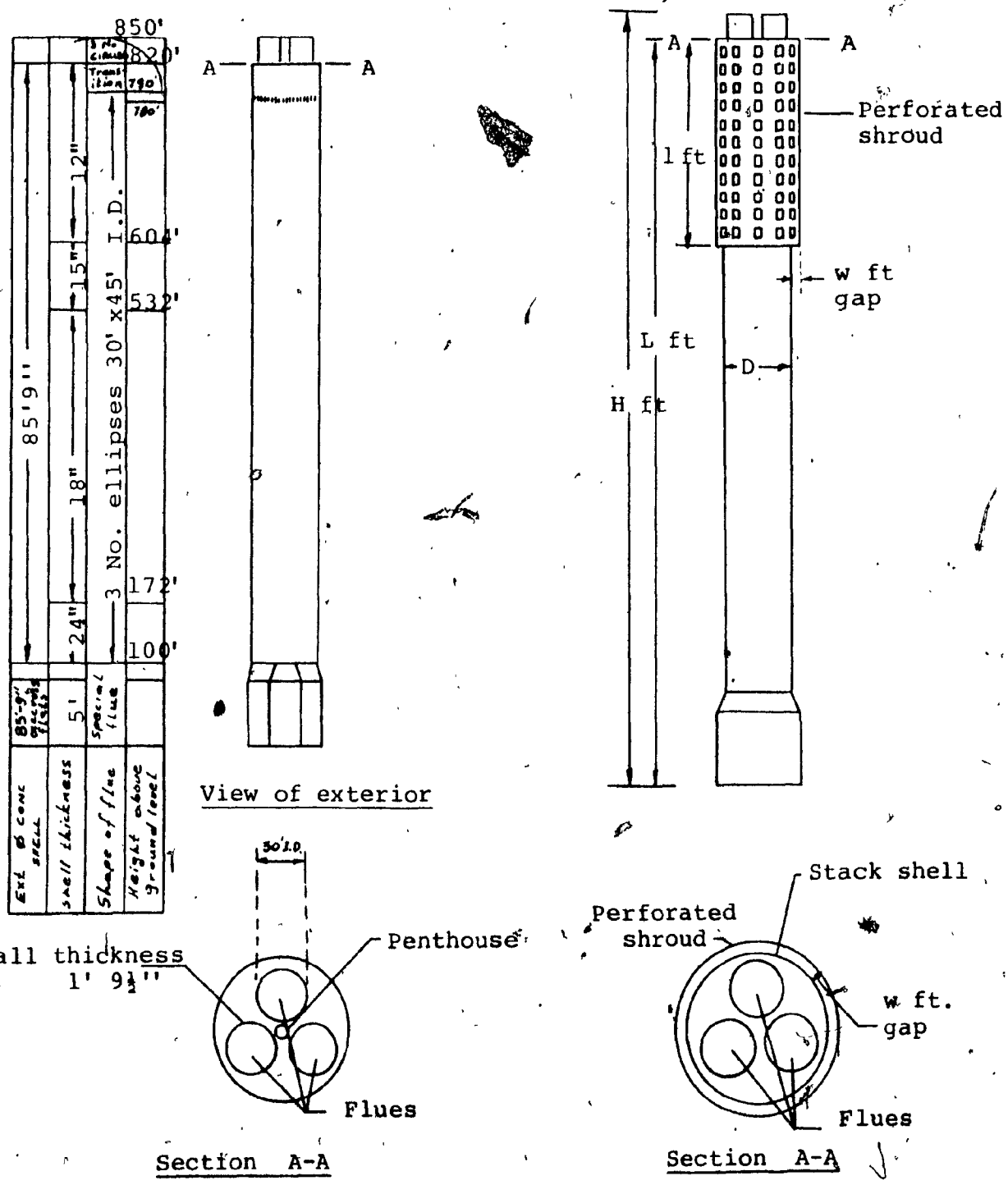

Illustration of the shroud system used in the Drax Power Station stack model.

Figure 5.1: Diagram of the stack for Drax Power Station.

In all, five types of shrouds were tested with dimensions as shown in the following table.

TABLE 5.1

Shroud Reference Number	PERFORATIONS		Length (l/L)	Gap (w/D)
	Length of the sides of the Squares (S/D)	Percentage open area		
1	0.0525	20%	0.25	0.117
2	0.0700	36%	0.25	0.117
3	0.0700	36%	0.125	0.117
4	0.0700	36%	0.25	0.059
5	0.0816	49%	0.25	0.117

The results of the tested models with shrouds are plotted in figure 5.2 as shown, along with the characteristics of the

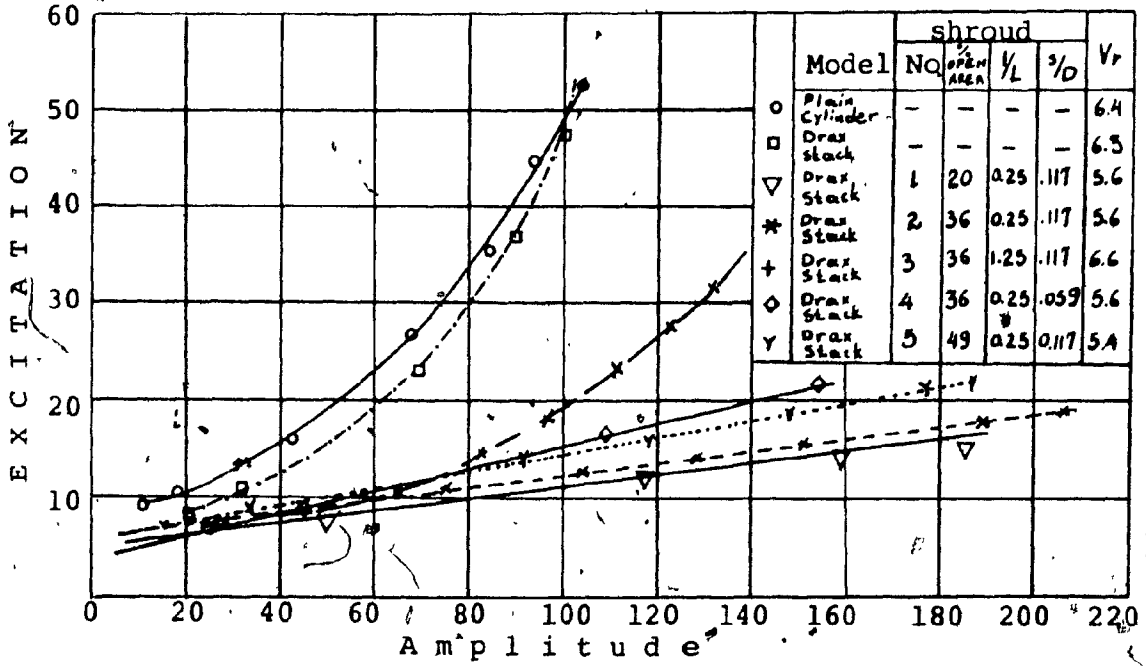

Figure 5.2: Variation of maximum amplitude in the cross-wind direction with damping.

shrouds and the reduced velocities (V_r) for maximum excitation. Shroud No. 1 proved to be the most effective but was only marginally better than shroud No. 2.

However, shroud No. 5 was less effective than No's 1 and 2 thus indicating that shroud effectiveness decreases considerably beyond an open area of 20%.

Comparison of the results for shrouds No. 3 and 4 reveals that greater stability results from increasing the length of shroud from $l/L=0.125$ to $l/L = 0.25$. Finally, increasing the gap width from $w/d = 0.059$ to 0.117 as in cases 2 and 4, improved stability. In addition to these observations, none of the models demonstrated any tendency to oscillate in the wind direction in the wind speed range $0 < V_r < 4$ even with values of structural damping as low as $\xi = 0.7$.

The investigation was continued in a turbulent wind flow with an extensity of turbulence $\frac{\bar{u}^2}{V} = 0.055$. The results are plotted in Figure 5.3, for the plain stack and for the stack fitted with shroud No.1. It may clearly be seen that for the same values of structural damping, the amplitudes of oscillation of the stack model fitted with shroud are considerably lower than those for the plain stack.

The drag coefficient of the shrouded stack was found to have little dependence on Reynolds number and to be about 0.9.

Similar experimental studies conducted by Knell[17] and by Wootton and Yates[18] indicates comparable results.

Based on these experimental results a stack configuration fitted with shrouds may be suggested as an effective means of reducing wind induced aerodynamic instability.

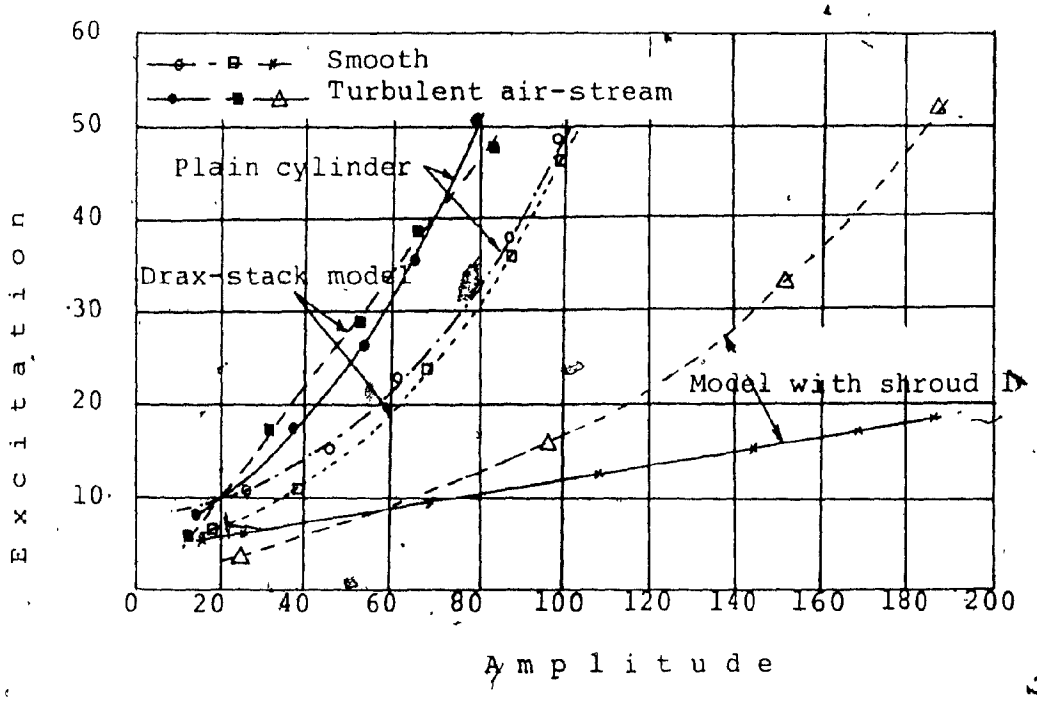

Figure 5.3: Variation with damping of maximum amplitudes in the cross-wind direction. Smooth and turbulent air-stream.

The proposed configuration is illustrated in Figure 5.4. Here, it is worth mentioning the fact that further experimental work is required towards improving and refining the present state of practice regarding the design of perforated shrouds.

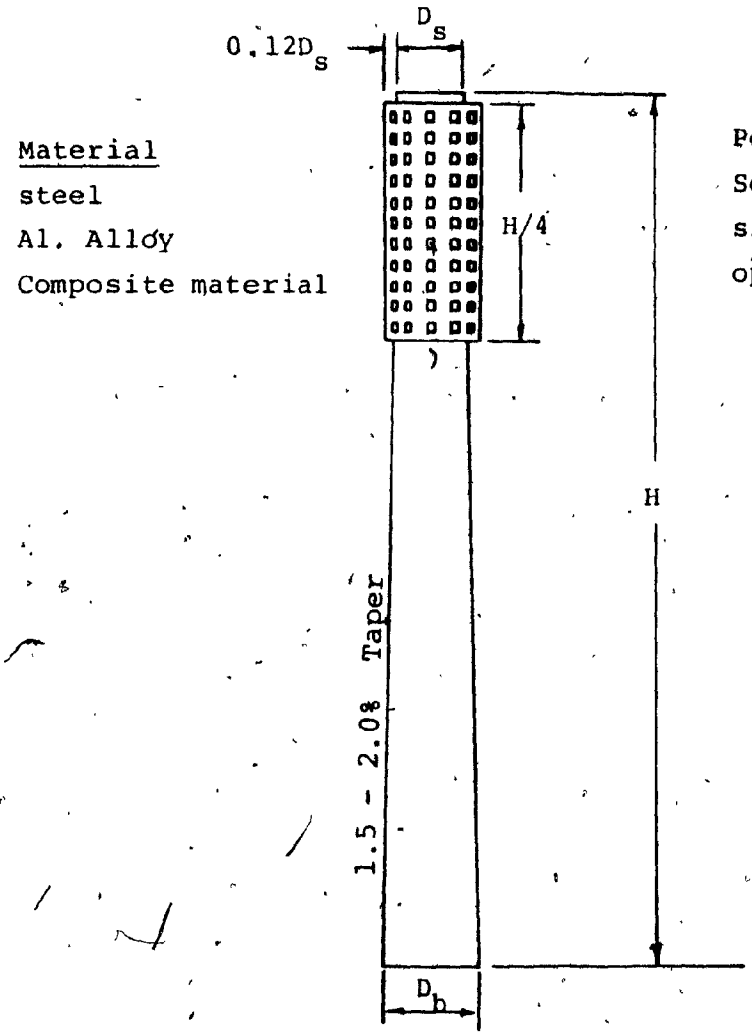

Material
steel
Al. Alloy
Composite material

Porous shroud
Square perforations of side length about 0.07D
open area ratio 20-36%

$H/D_s > 10.0$

Figure 5.4: Variable section self supported stack fitted with shroud.

5.2 HELICAL STRAKES

Helical strakes as means for reducing wind - induced instability in steel stacks have been introduced firstly by Scruton and Walshe[11] following an extensive experimental study.

They have shown in effect that it is possible to prevent extensive lateral oscillations by considering the use of these devices. The study was concluded by a final configuration of a stack system featuring a three start helix with a linear pitch of about 15 diameters but for several heights of strake.

Following this, further experiments by Woodgate and Maybrey [12], Cowbrey and Laws[13] as well as the continuation of the original work by Scruton[49], investigated the effects of varying the number, pitch, and height of strakes in achieving the most effective configuration.

The observations of these experiments may be summarized as follows.

For sub-critical values of Reynolds number ($Re<2 \times 10^5$), the drag of the cylinder fitted with strakes of height h=0.02D was approximately the same as the drag of the plain cylinder.

The effect of increasing the height of the strakes to h=0.036D was an increase of the initial drag coefficient by 0.15 - this increase being independent of the value of the Reynolds number.

In Figure 5.5, the values of drag coefficient (C_D) based on the diameter of the plain cylinder, are plotted against Reynolds numbers.

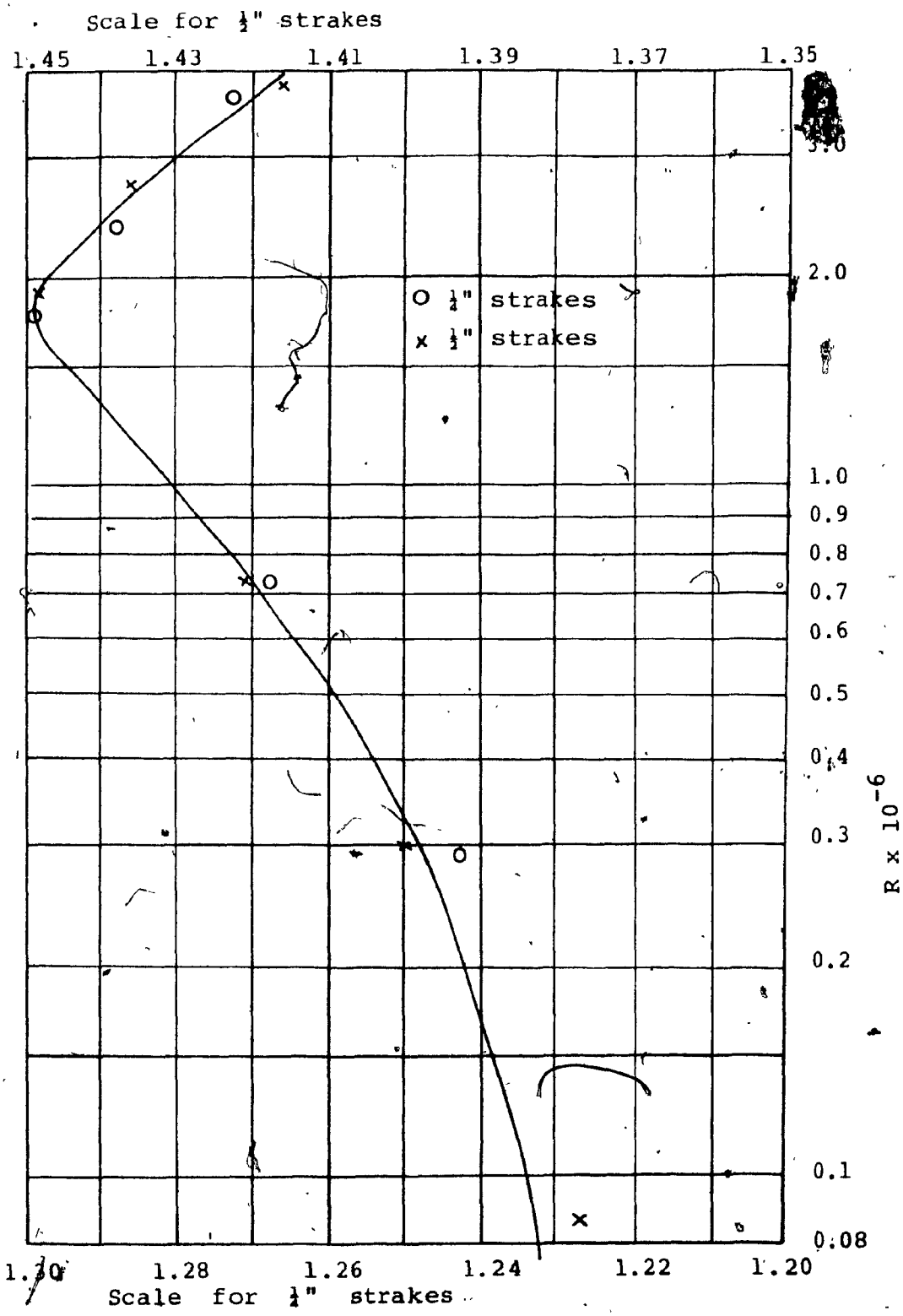

Figure 5.5: Drag coefficient of a circular cylinder with three helical strakes.

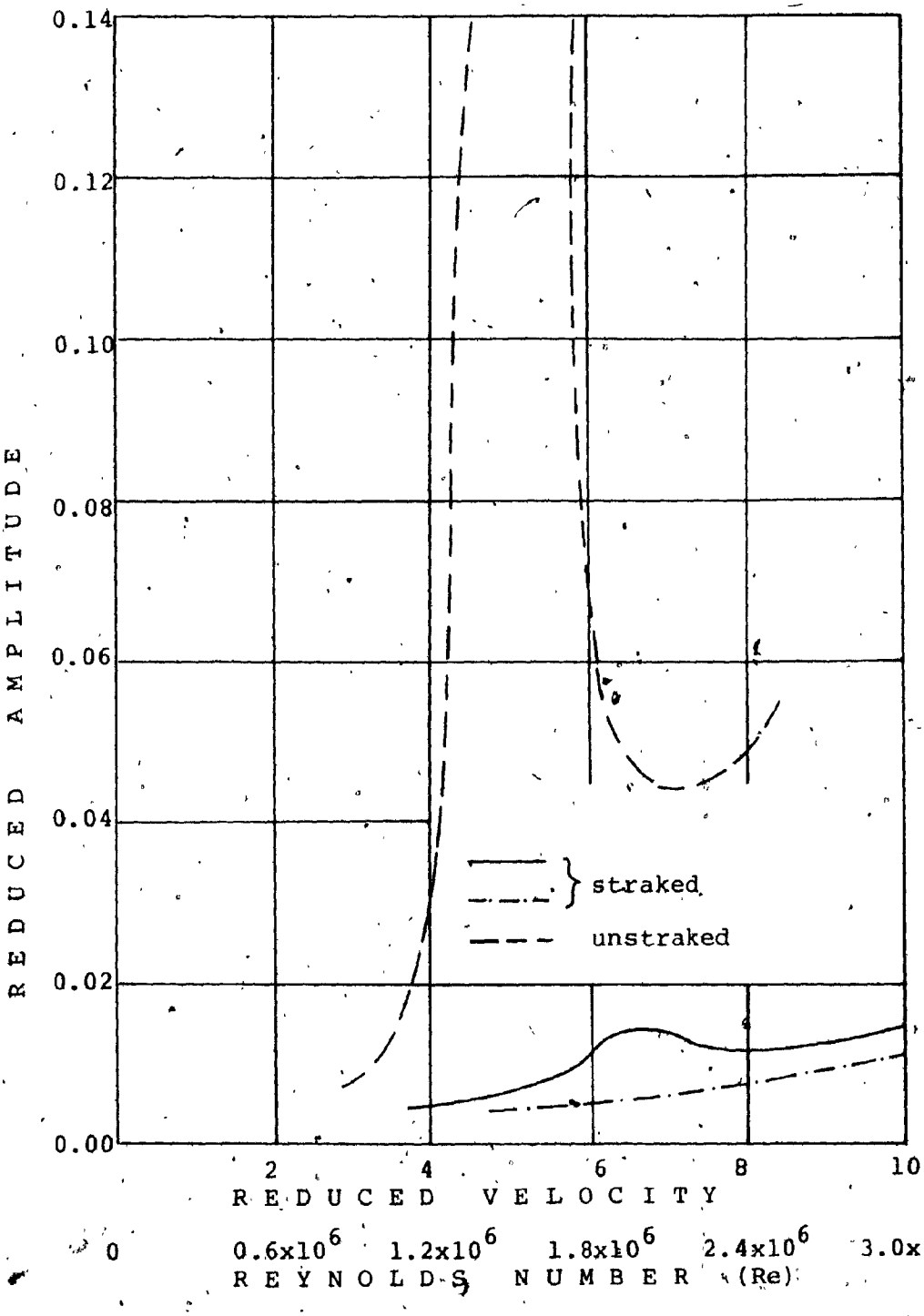

Figure 5.11: Comparison of a straked and unstraked rough surface stack L/D=11.5

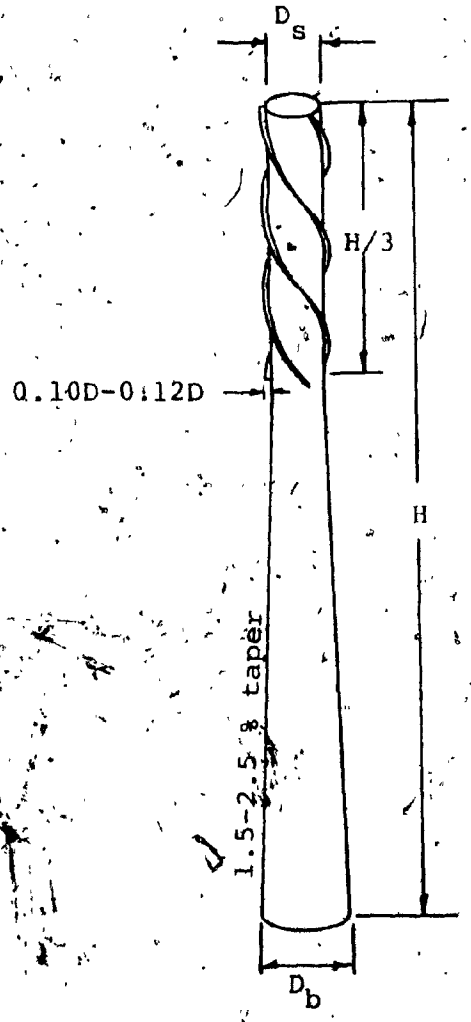

Helical strake

3-start helical strake

(sharp edged)

pitch=1 revolution in $5D_s$

Figure 512: Helical strake as means for suppressing wind induced oscillations

5.3. SPOILERS

Spoilers, as they are refered in the aerospace industry, are devices that spoil or reduce the lift on a lifting surface.

They have practical uses as ailerons for lateral control or as a lift control in the case of gliders to vary the aspect ratio (L/D).

Due to their effectiveness in lift control, they were first considered as means of spoiling the flow around circular stacks in Czechoslovakia by Novak.[20]

Prior to this, the only attempt in experimenting with devices closely resembling spoilers, as they are defined in aerodynamics literature, was made by Woodgate and Maybrey. The tests involved several strake configurations to determine the influence of a discontinuous strake.[12] Gaps were left in the strakes that were all the same and equal to the cylinder diameter.

However, it was shown that the configurations with gaps ware more unstable than with the continuous strake.

Wind tunnel tests were conducted by Novak[51], indicated that their effectveness was very favorable, especially in the subcritical range of Reynolds numbers. In the supercritical range, with increasing wind velocity, the amplitudes were approaching those obtained from a cylinder without spoilers.

These tests, being inconclusive, due to lack of experimental data sufficient to establish design criteria, were taken into consideration by Marten[52], in the design of

the Bukova hora television tower and latter, the Sucha hora tower.

The Bukova hora tower is 180 m high and is located in an area where relatively high winds are present, in Central Bohemia, Czechoslovakia. Various steel - sheet spoilers were fitted and full scale measurements obtained.

Theoretically, the effect of spoilers on the aerodynamic response of stacks with circular cross section may be explained from first principles, i.e the fluid flow past a circular cylinder.

As already discussed in Chapter 3.0, the von Karman vortex street produces periodic lateral forces thus inducing lateral oscillations.

The introduction of a spoiler sheet however, as shown in Figure 5.13, results in the break-up of the otherwise uniform fluid flow with the net result of increased drag component and negative lift net force.

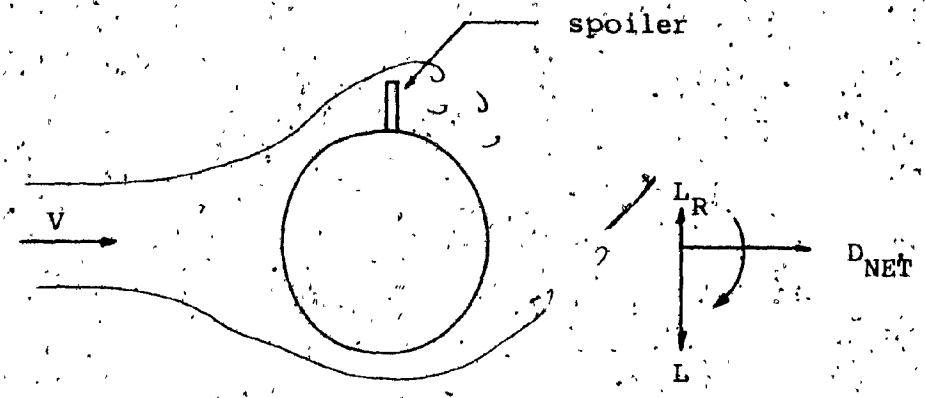

Figure 5.13: Flow past a circular cylinder with attached spoiler.

The drag component D_{NET} consists of the cylinder drag (D_C) and the drag of the attached spoiler (D_S)

Hence $$D_{NET} = D_C + D_S \qquad (5.1)$$

Depending on the geometry of the spoiler, D_{NET} could be 1.5 - 2.5 times the cylinder drag.

The alternating lift force (L) in a circular cylinder without spoiler is nearly equal and periodic.

With the introduction of a spoiler, the lift remains almost unchanged (L) on the one side, while it reduces to L_R on the other and at the same time the periodicity changes.

The torsional parameter (T), which is otherwise small, with the introduction of a spoiler increases considerably.

If, instead of a single spoiler, a system of small thin-sheet spoilers is attached along the height of a stack, the overall effectiveness can be increased considerably.

Such an arrangement would be independent of wind direction, would further reduce the lift forces by the non-uniform break up of the flow on both sides of the stack, would reduce wind induced torsion and the only negative effect would be a marginal increase in drag force inducing in- line oscillations. Theoretically, it is nearly imposible to accurately design a spoiler system simply because the behaviour of the flow cannot be clearly defined due to irregular interactions of the adjacent spoilers.

However, experimentaly, it may be possible to establish

fairly accurate design details. This would be possible by wind tunnel testing of various configurations.

Based on existing experimental data[51],[52], a configuration may be proposed featuring reduced lateral oscillations with no appreciable increase in drag coefficient (C_D).

This configuration as illustrated in Figure 5.14, consists of thin sheet spoilers with relative height of 0.165D and relative width of 0.270D. They are attached normal to the stack surface at centreline spacing of 0.235D so as to wind helically along the smooth part of the stack. The pitch of the winding is about 5.65D.

Preliminary performance evaluation of the effectiveness of a system such as described above, has been extremely encouraging due mainly to their advantage that although they reduce the lift coefficient C_D, as in the case of helical strakes, on the other hand the drag coefficient is about the same of that of a stack with perforated shrouds and lower of that of a stack with helical strakes.

No further studies were contucted on this subject and it is almost certain that a complete experimental program would lead into considerable improvements of their practical usefulness as a very effective means for suppressing wind induced oscillations.

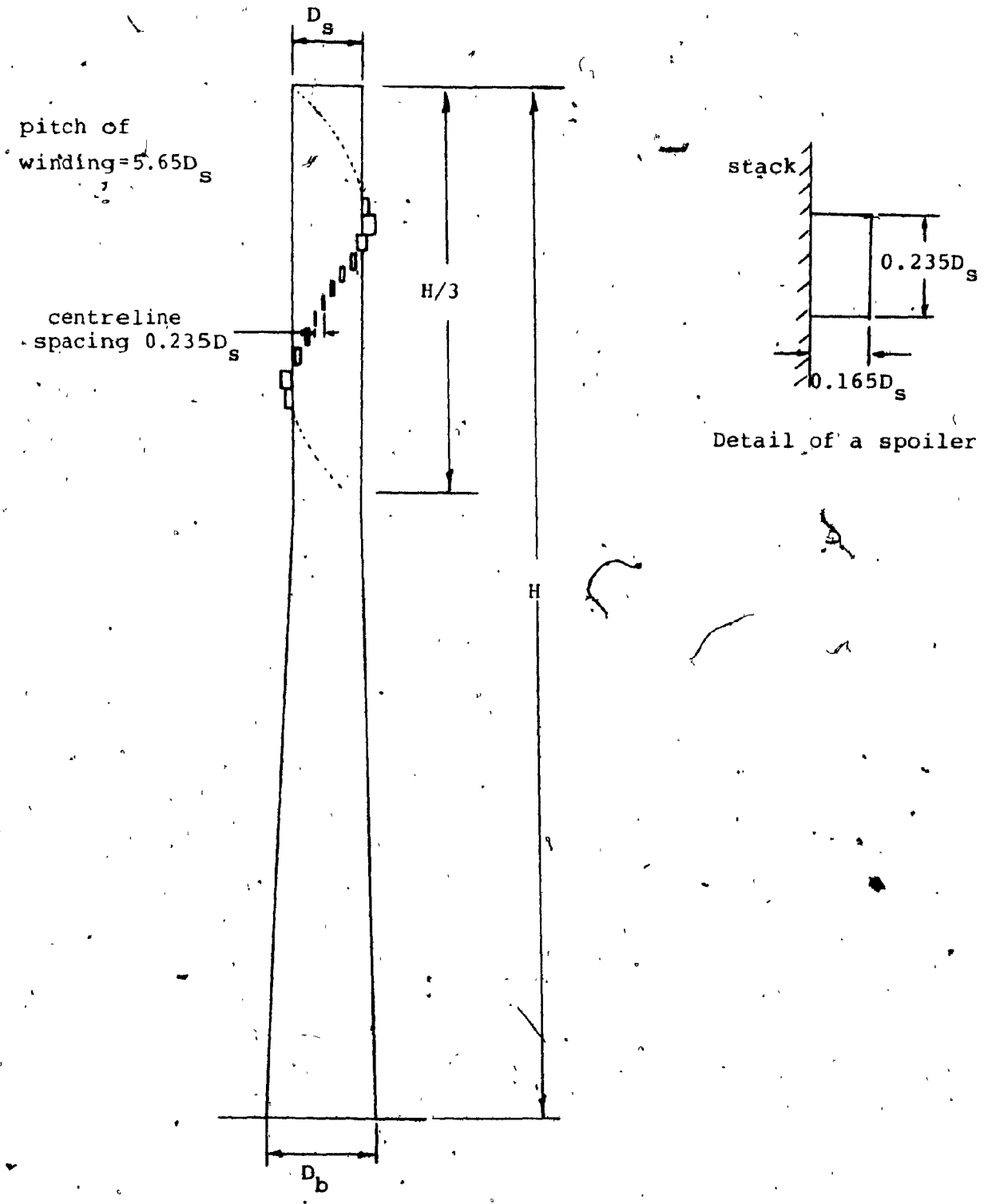

FIgure 5.14: Illustration on the use of spoilers on a self-supported stack.

5.4 UNI-DIRECTIONAL DEVICES

Another type of aerodynamic device that was suggested by Baird[53] as an effective means of reducing wind-induced vibration of pipeline bridges takes the form of saw-tooth fins, fins or splitter plates which reduce vortex induced oscillations by interfering with the exchange of fluid access the wake, as illustrated in Figure 5.15.

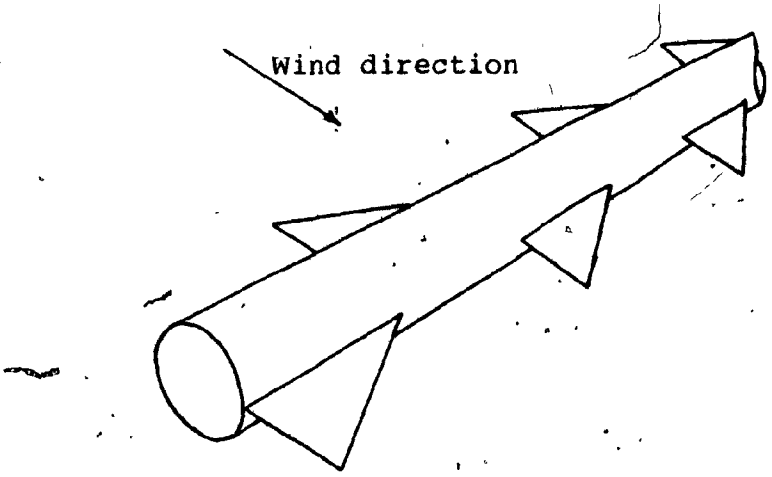

Figure 5.15; Saw - toothfins on a pipeline suspension

However, these devices are mostly uni-directional and are only effective when the flow from a particular direction needs to be considered therefore, the only practical use may be in pipeline suspension bridges.

In steel stacks, unless the predominant wind direction is well defined, the use of these devices may be innapropriate.

In addition to above, another type of aerodynamic device was considered, namely an airfoil.

It is well known that a symmetric airfoil of the type

suggested by Joukowski[54] when subjected to fluid flow at zero angle of attack and for low Mach Numbers (up to 0.25) has zero lift and drag coeficient. This means that the exciting forces are non-existent.

This, of course holds only at zero angle of attack -that is, when the chord-line is parallel to wind direction.

Given the fact that the design wind speed of a stack is always less than M=0.25 this device may be highly efficient if it is set always in the proper direction as described above. This may be achieved if it is designed in such a manner as to be freely to rotate about its aerodynamic center which may be located forward of the center of gravity in order for the applied moments to prevent it from diverting from any other than zero angle of attack.

The major flaw to such a system would be possible failure or jamming of the mechanical system with the net result of creating high drag and lift coefficients with catastrophic results. Figure 5.16 illustrates the proposed system.

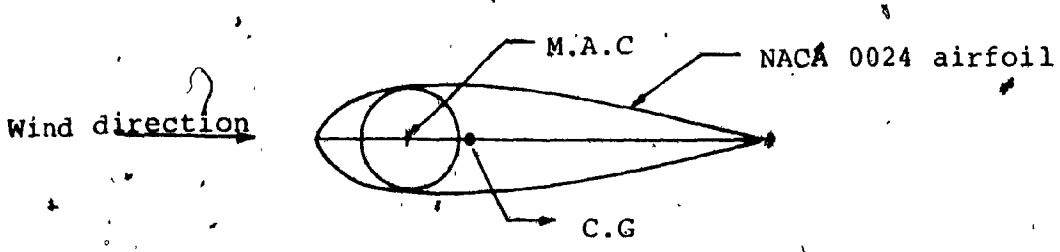

Figure 5.16: Cross section of a cylindrical stack fitted with a NACA airfoil.

CHAPTER 6

DAMPING DEVICES

6.1 DAMPING EFFECT

Positive damping characteristics which act against the motion in limiting the amplitudes of such motions by dissipating such energy effects as friction, viscous resistance, or internal deformation in the material, are present in steel stacks.

However, situations may arise where the motion itself creates a force which actually supports the motion. When this happens on a structure due to its movement relative to the wind, it is known as aerodynamic instability or negative aerodynamic damping.

Positively and negatively damped free vibrations have already been described and illustrated in Figures 4.2 and 4.4.

Due to the dependence of amplitudes of oscillation on the structural energy - absorption quantities, increasing the mass of a stack may not be totally beneficial.

The increase may produce a reduction in the natural frequency and hence in the wind speeds at which oscillations due to vortex shedding will tend to occur. It is thus possible that the addition of mass may reduce the critical speed in a certain mode from a level outside the actual design wind-speed range to a level within it.

It has been found[50] that, if additional mass is used to limit amplitudes of oscillation in the fundamental mode of a stack, the most effective position for the added mass is at the top. Such action may lower the frequency of the

second mode and result in an increased risk of instability in the mode. Therefore, it would be more advantageous to incorporate the mass near the upper nodal point of the second mode so that the frequency of oscillation remains unnaffected. The additional mass however, may be more beneficial if it is stressed during the motion so that it also contributes to the structural damping.

The structural damping forces, resulting from the structure dissipating energy during vibration, are proportional to the velocity of motion. In practice, apart from positive damping due to hysteresis, representing the energy absorbed by the internal friction of the material in terms of the stress/strain relationship forming a closed loop under cyclic loading, energy is also absorbed in sliding at joints and at the foundations [59].

These additional effects may result in an increase in structural damping with increasing amplitude and hence may limit the aerodynamic indiced motion.

However, the effects of friction in stack linings may dominate the structural damping but cannot be calculated. Structural damping may be possible to measure only once the construction of the entire stack has been completed.

The stack may be set in motion by pulling the top with a cable and then releasing.

Another method that has been used in fairly tall stacks is the firing of rockets sequentialy at the top of the

structure. The decay from which the logarithmic decrement of damping (δ) can be calculated, can be recorded using standard transducers. The importance of increasing damping is illustrated in Figure 6.1.

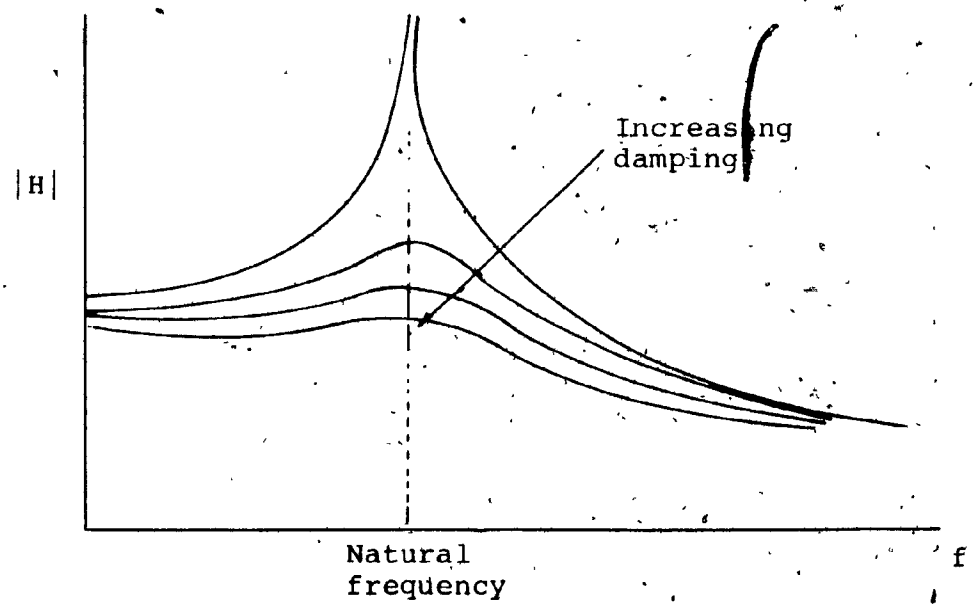

Figure 6.1: Magnification of static deflection vs natural frequency.

Various methods of increasing the structural damping have been developed in the form of mechanical devices, the most important of which are the following:

(i) Active Mechanical Dampers: These devices produce a force on the stack that opposes the fluid dynamic force so that no appreciable oscillation will occur. The layout of such a system is shown in Figure 6.2. The aerodynamic force is sensed by an accelerometer on

the top of the stack and the signal from this controls the swinging of a mass. The entire system seems to be very complex and there must be safeguards to ensure that the mechanical force does not act in - phase with the aerodynamic forces, thus increasing the amplitude of oscillation. Such a system requires careful maintenance and although it has been fitted to full scale stacks, it has not always been successfull. A major drawback is its reliance on electric power. It has been observed that power supply failure would most likely occur during a storm when high velocity winds are present and thus a damping device is mostly needed.

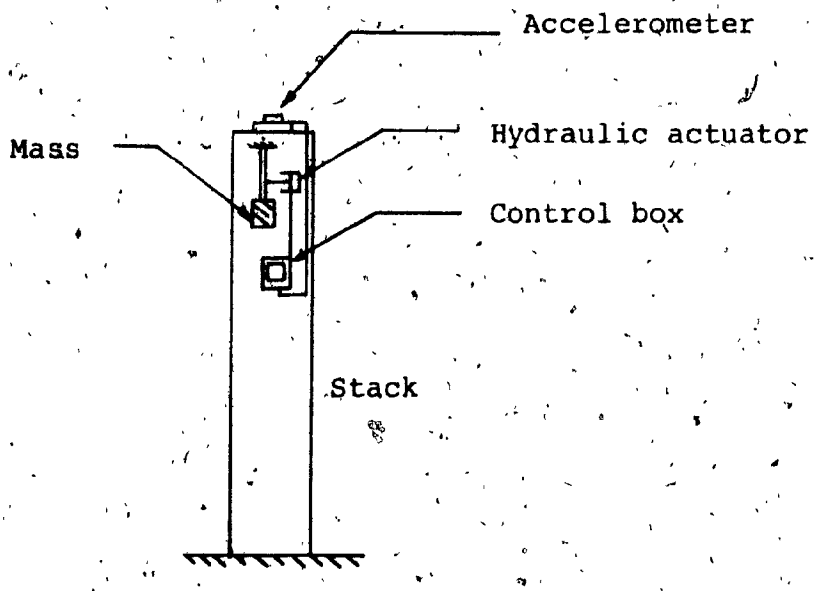

Figure 6.2: Schematic diagram of an active mechanical damper on a stack.

(ii) Impact Dampers: The best known damper is the chain type which is illustrated in Figure 6.3. It consists of a chain in a rubber sleeve suspended so that it can impact against a vertical channel. This process absorbs the oscillating energy to a degree that is dependent on the oscillation frequency [55].

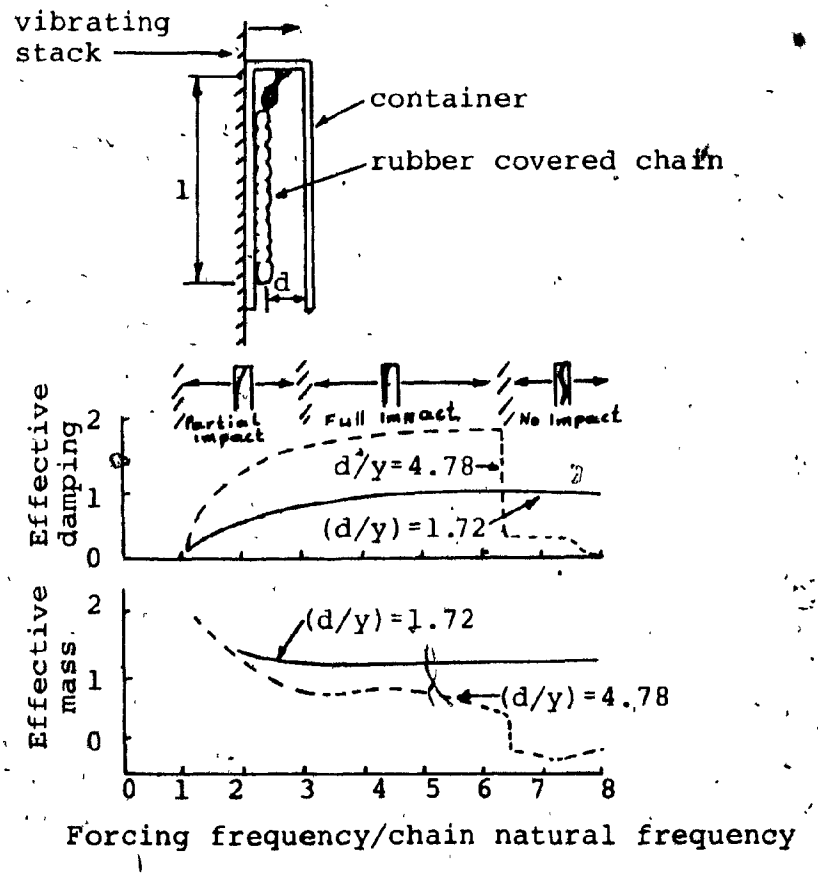

Figure 6.3: Response of a chain impact damper.

The effects of various parameters on the performance characteristics of such a damper have been determined experimentally[55] and chain dampers were fitted succesfully to a 20 meters high missile, which would

otherwise be vulnerable to wind action in its launch position. The dampers in this particular case weighed about 50% of the total weight of the missile and increased the damping by a factor of three except at small amplitudes the effect was incignificant.

Actually, at these small amplitudes, the chain failed to touch the channel and there was no effective increase in damping. The amount of energy absorbed by the chain dampers remains a maximum over a limited frequency range and if the ratio between the frequencies of the various modes of a structure is greater than about three, additional dampers will be required to increase the effective frequency range.

(iii) Tuned Dampers: These devices consist of a small mass-spring damper system fitted near the top of the stack and tunned to absorb considerable energy. The energy absorbed by the small mass is equal to the product of the force and the displacement. Thus, to absorb a large percentage of the energy generated by the structure, it is necessary for the secondary mass system to have considerable freedom to move. However, their disadvantage as a solution to the chimney stack problem is the need for periodic maintenance along with possible mechanical failures.[56],[57], [58].

(iv) Rubber and Spring Dampers: A major portion of the energy generated during aerodynamic excitation of a stack, is absorbed by the foundations and soil under the foundations.

Thus, it is very important to provide energy absorbing conditions at the foundation level.[59]

Since it is rather difficult to define the damping properties of the soil within a reasonable degree of accuracy, and since the energy absorbing capabilities of the soil are limited, the need for an alternative method became aparent.

Recent investigations by Goodyear Rubber Co. indicate that it is possible to increase structural damping by using rubber as lateral supporting material at the base of the stack. Figure 6.4 illustrates a typical configuration.

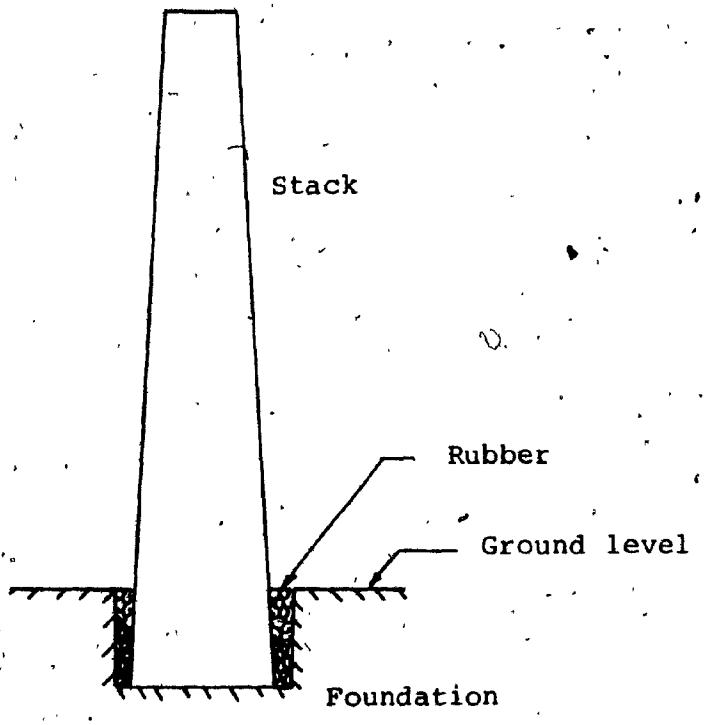

Figure 6.4 Damping of stack with rubber dampers.

Rubber, an elastomeric material, excibits very high resilience characteristics, i.e. capacity to store energy. Resilience is defined as the ratio of energy output to energy input. Due to the fact that some input energy is always lost through internal friction, resilience values are always less than 1. The loss of energy in the form of frictional heat is knowing as hysteresis and it is a major contributing factor in damping effect. The use of rubber as damping medium seems promising, however, the only drawback seems to be its susceptibility to high temperatures present and or its reduced effectiveness in very low temperatures.

As an alternative to rubber may be considered the use of conical springs.

These springs are a specialized variety of the conventional helical - compression spring and may be used in the same mahner as rubber to laterally support the stack and provide damping.

The major advantage, however, of the spring over the rubber is its mechanical properties.

The conical spring can be designed so that each coil nests wholly or partially into the adjacent larger coil so that the solid height of the spring can be as small as one wire diameter [60] Conical springs can be designed with a controled increasing rate as each turn succesively becomes innactive during deflection. The feature may be utilized as vibration damper. By using variable-pitch turns the spring can be designed to a variable frequency since the exciting force is at a single frequency. This is its greatest adva-

ntage as the frequency of the mass-spring system, being variable, is far from the disturbing frequency.

The filtering of disturbing forces may be calculated as

$$\% \text{ of force transmitted} = \frac{1}{\left(\frac{n_D}{n}\right)^2 - 1} \times 100$$

where n_D is the frequency of the disturbing force i.e. the frequency of the oscillating stack and n is the natural frequency of the spring-mass system. In Figure 6.5, a layout of a spring damping system is shown along with pertinent data concerning conical springs.

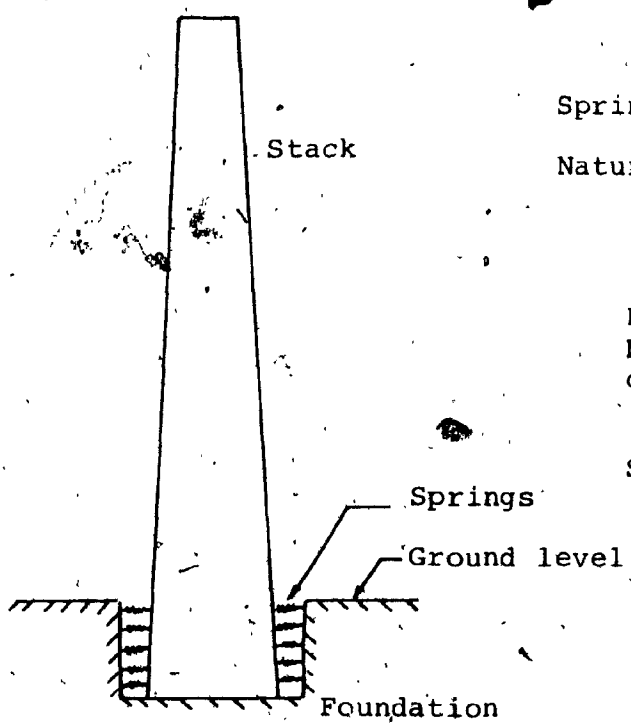

Spring rate K_s = Load/ Deflection

Natural frequency of spring

$$f_n = \frac{13{,}900d}{ND^2} \text{ cps for steel}$$

N Number of coils
D Spring variable diameter
d wire diameter

Spring index $c = \frac{d}{D}$

Figure 6.5 Springs as damping device on a stack.

CHAPTER 7

CONCLUSIONS

7.1 CONCLUSIONS

As stated in the introduction, the purpose of this study was to investigate the effectiveness of several devices in suppressing wind induced vibrations in steel stacks.

A number of possible sources of vibration were also discussed in determining the critical mechanisms of wind induced excitations.

Based on experimental results, it was possible to determine the influence of various aerodynamic and damping devices in the dynamic behaviour of steel stacks under wind action.

In comparing the aerodynamic devices examined, the following observations may be drawn:

(i) Strakes, though more effective in reducing oscillations, have the disadvantage that the drag is very much greater than that of a plain circular stack at high Reynolds numbers. In terms of the non-dimensional drag coefficient, straked stack C_D= 0.4 to 0.6 while for a typical straked stack C_D= 1.4, where C_D is based on the stack diameter as indicated in figure 7.1

(ii) Tests on model stacks at low Reynolds numbers indicated that the smoke (or other effluent) disposal was assisted by the use of shrouds and marginally by the use of strakes. The difference in plume paths when the efflux to free-stream velocity was 0.5 was considerable. The

The effluent, it was found, was dispersed most effectively at velocity ratios as low as 0.25. However, at velocity ratios above 1.0 there was little difference between the dispersal characteristics of both models.

(iii) Spoilers, although at the experimental stage, seem to posess some very interesting characteristics that may be advantageous over other aerodynamic devices. The break up of the uniformity of flow past a circular stack is achieved in an unlike manner due to the discontinuity of the spoilers thus encouraging vortex shedding at a wide range of frequencies rather than a single

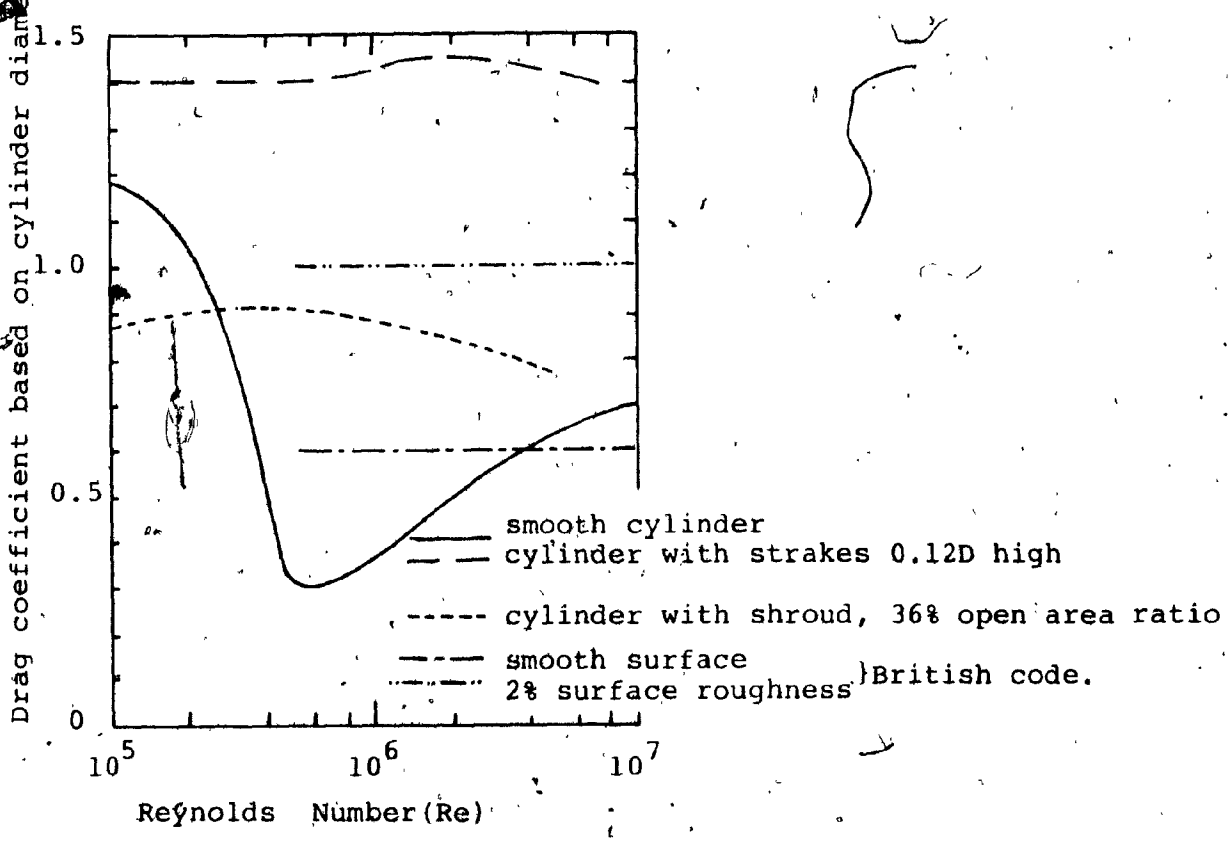

Figure 7.1: Drag coefficient of a circular cylinder.

frequency.

Limited experimental results indicate that the drag coefficient in spoilers ranges from C_D 1.1 to C_D 1.25 that is slightly lower than that of strakes.

As a lift control devices seem to be equally effective as strakes and somehow better than shrouds. To this point it is not possible to further assess the effectiveness of spoilers as the experimental results available are not sufficient enough to establish adequate design criteria. However, it appears that if proper experimental investigation is carried out, it may lead to very interesting findings from the point of view of the structural engineer.

(iv) As to the other devices mentioned, namely fins and airfoils, they seem highly advantageous in theory by not likely applicable in practice due to serious flaws in being either susceptible to wind direction or exposed to mechanical failure. Further research may clarify further their feasibility.

(v) In investigating the usefulness of the damping devices the findings may be summarized as follows.

Damping became a serious problem with the introduction of lightweight materials and the considerable increase in height of modern steel stacks.

Almost all mechanical dampers fitted on or near the top of the structure are highly volnurable to mechanical failure and present difficulties in maintenancing

these devices. Hence, due to high probability of failure, their beneficial effect may bot be taken fully into consideration at the design stage.

Due mainly to the highly contributary effect of the foundations in structural damping, it seems that spring or rubber dampers as proposed at the foundation level may contribute to an appreciable increase in damping comparable to that or better than all other mechanical dampers with the added advantage of high degree of reliability and reduced maintenance. This, of course, could only be achieved if further research is carried out, both theoretical and experimental. Especially the use of springs as dampers seems highly promising due to some interesting properties of the springs, namely the variation of the spring frequency due to the exciting force thus preventing resonance of the spring.

(vi) Finally, the use of guy wires as already has been discussed is a good method of increasing the natural frequency of the stack as well as the structural damping. As the stack deflectes under the influence of lateral loading (wind load) some of the guys are extended and friction between the strands absorbs energy. The magnitude of the effect is difficult to assess and clearly depends on the degree of guy movement associated with

each mode shape. Clearly, the major dissadvantage of guy wires is the vulnerability of the guys themselves to aerodynamic excitation. In particular, ice formation can change an otherwise stable shape into one that suffers from galloping, although some ice-free stranded cables have also oscillated.

7.2 FUTURE WORK

As stated in the conclusions above, further research is needed to define and further refine the effectiveness of the aerodynamic devices under consideration.

Given the fact that quantitative information on many aspects of vibration is sparse, more research is needed to provide reliable data on which to base future designs, so as to avoid structural instability and to indicate preventive action if it occurs.

In concluding the present study the following subjects have been found to be of prior importance in requiring further investigation.

- The influence or Reynolds number on excitation.
- The influence of taper on excitation of stacks
- The effect of adjacent structures on excitation
- Structural damping observed from field experiments
- Gust response of structures.
- Further experimental investigation of aerodynamic devices
- Case histories with quantitative observations

Finally, in view of the above, the seriousness of the problem

requires prompt attention from both the researches and the State as it is vital to human health and safefy.

REFERENCES

REFERENCES

[1] Société de Diffusion des Techniques du Bâtiment et des Traveaux Publics, "Règles définissant les Effects de la Neige et du Vent sur les Constractions," Règles N.V. 65 Revisées 1967 et Annexes, 9Rue la Perouse, Paris, 16 iéme.

[2] Société de Diffusion des Techniques du Bâtiment et des Traveaux Publics, "Circulaire du 24 Novembre 1970 parrue au Journal Officiel du 13 Décembre 1970", 9 Rue la Perouse París, 16 ième.

[3] Dockstader, E.A., and Swiger, W.F., "Resonant Vibration of Steel Stacks", Proc. ASCE, Separate No. 541, Vol. 80, November 1954, pp. 1-27.

[4] Dickey, W.K., and Woodruff, G.B., "The Vibrations of Steel Stacks", Trans. ASCE, Vol. 121, Paper No. 2831, pp. 1054-1087, 1956.

[5] Sharma, C.G., Johns, D.J., "Wind - Induced Oscillations of Circular Cylindrical Shells:An Experimental Investiqation". Report TT7008, Loughborough University of Technology, July 1970.

[6] Davenport, A.G., "The Wind - Induced Vibration of Guyed and Self-Supportive Cylindrical Columns", Transactions of the Eng. Institute of Canada, Vol. 3, No. 4, Dec. 1959, pp. 113-141.

[7] Vickery, B., Watkins, R., "Flow-Induced Vibrations of Cylindrical Structures", Proc. 1st. Conf. on Hydraulics and Fluid Mech., Pergammon Press, New York, 1962.

[8] Scruton, C., "On Wind-Excited Oscillations of Stacks, Towers and Masts", Proc. Int. Conf. on Wind Effects on Buildings and Structures, National Physical Laboratory, London, 1965.

[9] Ferguson, N., Parkinson, G.V., "Surface and Wake Flow Phenomena of Vortex-Excited Oscillations of a Circular Cylinder", ASME Journal of Engineering for Industry, Vol. 89(1), Nov. 1967, pp. 831-840.

[10] Novak, N., Tanaka, H., "Effects of Turbulence on Galloping Instability" Proc. ASCE, Eng. Mech. Div., Vol. 100, No. EM1, February 1974, pp. 27-47.

[11] Scruton, C., Walshe, E.E.J., "A Means for Avoiding Wind-Excited Oscillations of Structures with Circular or Nearly Circular Cross Section", National Physical Lab., Aero Report 335, Teddington, 1957.

[12] Woodgate, L., Maybrey, J.F.M., "Further Experiments on the use of Helical Strokes for Avoiding Wind Excited Oscillations of Structures with Circular or Near Circular Cross-Section", National Physical Lab., Aero Report 381, Teddington, June 1959.

[13] Cowdrey, C.F., Lawes, J.A., "Drag Measurements at high Reynolds Numbers of a Circular Cylinder Fitted with Three Helical Strakes", National Physical Lab., Aero Report 384, Teddington, July 1959.

[14] Walshe, D.E., Cowdrey, C.F., "The use of Aerodynamic-Stabilizing Strakes on Chimney Stacks Supporting Pipes" National Physical Lab., Aero Report 1310, Teddington, February 1970.

[15] Price, P. "Suppression of the Fluid-Induced Vibration of Circular Cylinders", J. Eng. Mech. Div. Proc. ASCE, Paper 1030, 1956.

[16] Walshe, D.E., "Wind-Excited Oscillations of Groups of Four Rods of Circular Cross Section", National Physical Lab., Aero Note 1072, Teddington, Sept. 1968.

[17] Knell, B.J., "The Drag of a Circular Cylinder Fitted with Shrouds", National Physical Lab., Aero Report 1297, Teddington, May 1969.

[18] Wootton, L.R., Yates, D. "Further Experiments on the Drag of Perforated Shrouds", National Physical Lab., Aero Reprot 1321, Teddington, July 1970.

[19] Novak, M. "The Influence of Spoilers Upon the Drag Force of Cylinders" Dynamika Stowebnich Konstruckci, 111. dil, Praha 1961 pp.265-304 (in Czechoslovak)

[20] Novak, M. "The Influence of Spoilers Upon the Drag Force of Cylinders" Stowebnicky Casopis, Bratislava 1966 (unpublished)

[21] Korenev, B.G., Syssoev, V.1. "Metod gasheniia Kolebanii Sooruzhenii Bashennogo Typa", Bulleten Stroitelnoi Techniki, N5, 1953. (In Russian)

[22] Korenev B.G. "Some Problems of Dynamic Design of Elastic Structures, Equipped with Dampers for Wind Effects on Buildings and Structures", Tokyo, Japan, Saikon Co. Ltd. 1971.

[23] Walshe, D.E., Wooton, L.R. "Preventing Wind-Induced Oscillations of Structures of Circular Section" National Physical Laboratory, Teddington, England, Dec. 1970.

[24] Wong, H.Y. "An Aerodynamic Means of Suppressing Vertex excited Oscillation", Proc. Instn. Civ. Engrs, Part 2, Vol 63, Sept. 1977 pp. 693-699.

[25] Jensen, M., Franck, N. "Model - Scale Tests in Turbulent wind", The Danish Technical Press, Copenhagen, 1963.

[26] Harris, R.I. "Measurements of Wind Structure" Proc. Symposium on External Flows, Univ. of Bristol, July 1972.

[27] Davenport, A.G. "The Relationship of Wind Structure to Wind Loading", Int. Conf. on the Wind Effects on Buildings and Structures, National Physical Laboratory, Teddington, England, 1963.

[28] Counihan, J. "The Structure and the Wind Tunnel Simulation of Rural and Urban Adiabatic Boundary Layers", Proc. Symposium and External Flows, Univ. of Bristol, July 1972.

[29] Templin, R.J. "Interim Progress Note on Simulation of Earth's Surface Winds by Artificially Thickened wind Tunnel Boundary Layers" N.R.C., NAE-LTR-LA-22, Feb. 1969.

[30] Harris, R.I., "On the Spectrum and Autocorrelation Function of Gustiness in High Winds", Elect. Res. Ass. SP1/T14, 1963.

[31] Dalghliesh, W.A. "Statistical Treatment of Peak Gusts on Cladding", Proceedings of the Structural Division, ASCE, Sept. 1971.

[32] Dalgliesh, W.A. "National Building Code of Canada", 1975 Associated Commitee on the National Building Code, National Research Council of Canada.

[33] Davenport, A.G., Isyumov, N. "The Application of the Boundary Layer Wind Tunnel to the Prediction of Wind Loading" Paper No. 7, Proceedings of the International Research Seminar on Wind Effects on Buildings and Structures, Ottawa, Sept 1967. University of Toronto Press.

[34] Hoerner, S.F., "Fluid - Dynamic Drag",Pub. by Hoerner Fluid Dynamics, P.O.Box 342, Brick Town, N.J. 08723,1965

[35] Föppl, O., "Lift and Drag on Flat and Curved Plates", Jahrbuch IV der Motorluftschiff-Studiengesellschaft, Berlin 1911.

[36] Birkhoff, G.D., "Formation of Vortex Streets", Journal of Applied Physics, Vol. 24, no. 1, p. 98, 1958.

[37] Tritton,D.J., "Experiments on the Flow Past a Circular Cylinder at Low Reynolds Numbers", Journal of Fluid Mechanics, Vol. 6, p.547, Nov.1959.

[38] Humphreys,J.S., "On a Circular Cylinder in a Steady Wind at Transition Reynolds Numbers", Journal of Fluid Mechanics, Vol. 9, part 4, p.603.

[39] Roshko, A., "Experiments on Flow Past a Circular Cylinder at Very High Reynolds Number", Journal of Fluid Mechanics, Vol. 10, p.345,1961.

[40] Smith, J.W., Jonsson, A., "Browns Ferry Chimney", Proceedings of the American Society of Civil Engineers, Journal of the Power Division, June 1970.

[41] Maugh, L.C., Rumman, W.S., "Dynamic Design of Reinforced Concrete Chimneys", Proceedings of the American Concrete Institute, Sept. 1967, pp. 558-567.

[42] Sachs, P., "Wind Forces in Engineering", Pergamon Press, 1972.

[43] Walshe, D.E., "The Aerodynamic Investigation for the Proposed 850 ft High Chimney Stack for the Drax Power Station". NPL Aero Report 1227. National Physical Laboratory, Teddington 1967.

[44] Novak, M., "Model Study of the Dynamic Characteristics of Guyed Masts", Proc. Conf. on Exper. Methods of Investigating Stress and Strain in Structures, Building Research Institute, Prague, 1965.

[45] Parkinson, G.V., Brooks, N.P.H., "On the Aeroelastic Instability of Bluff Cylinders", J. Appl. Mech., Vol.28, 1961, pp. 252-258.

[46] Novak, M., "The Wind-Induced Lateral Vibration of Guyed Masts with Circular Cross Section", Proceedings Symposium on Tower-Shaped Steel and Reinforced Concrete Structures, Bratislava, 6-8 June, 1966, Edited by the Intern. Assoc. Shell Structures, Madrid, 1968, pp.169-188.

[47] Walshe, D.E.J., Whitbread,R.E., "Aerodynamic Investigation for a Stack for the Canada-India Reactor Project", Rep. NPL/Aero/395. National Phisical Laboratory, Teddington,1959

[48] Price, P., "Suppression of the Fluid-Induced Vibration of Circular Cylinders", J.Engng Proc. Amer. Soc. Civ. Engrs, Vol. 82, No. EM3, 1956, p.1030.

[49] Scruton, C., "Note on a Device for the Suppression of the Vortex-Excited Oscillations of Flexible Structures of Circular or Nearly Circular Section, with Special Reference to its Applications to Tall Stacks",NPL Aero Note 1012, National Physical Lab., Teddington, England, 1963.

[50] Nakagawa, K., et al. "An Experimental Investigation of Aerodynamic Instability of Circular Cylinders at Supercritical Reynolds Numbers", Wind Effects on Buildings and Structures, Symposium NPL, Teddington, England, 1963.

[51] Novak, m., "Nektere otazky spolupusobeni podlozi pri kmitani zakladu" V knize V. Kolouska a kol.: Dynamika stavebnich konstrukci, III. dil, Praha 1961, pp. 265-304. (in Czech.)

[52] Marten, J.,"Steel Structure of Central Bohemia Television Transmitter" Presented in the Symposium on Tower - Shaped Steel and Reinforced Concrete Structures, by the International Association for Shell Structures, Bratislava June 6th - 8th 1966.

[53] Baird, r.c., "Wind-Induced Vibration of a Pipeline Suspension Bribge and its Cure". Trans. Am. Soc. Mech. Engineers, Vol.77, pp. 797-804, August 1955.

[54] Jones, R.T., "Properties of Low Aspect-Ratio Pointed Wings at Speeds below and above the Speed of Sound," NACA TN 1032, March, 1936.

[55] Reed, W.H., "Hanging-Chain Impact Dampers: A Simple Method for Damping Tall Flexible Structures" Wind Effects on Buildings and Structures, International Research Seminar, Ottawa, Canada, 1967.

[56] Den Hardog, J.P., "Mechanical Vibrations", McGraw-Hill, New York, 4th Edition, 1956.

[57] Snowdon, J.C., "Vibration and Shock in Damped Mechanical Systems", Wiley and Sons, 1968.